Review article

Stefano L. Oscurato, Marcella Salvatore, Pasqualino Maddalena and Antonio Ambrosio*

From nanoscopic to macroscopic photo-driven motion in azobenzene-containing materials

https://doi.org/10.1515/nanoph-2018-0040
Received April 3, 2018; revised May 21, 2018; accepted June 26, 2018

Abstract: The illumination of azobenzene molecules with UV/visible light efficiently converts the molecules between *trans* and *cis* isomerization states. Isomerization is accompanied by a large photo-induced molecular motion, which is able to significantly affect the physical and chemical properties of the materials in which they are incorporated. In some material systems, the nanoscopic structural movement of the isomerizing azobenzene molecules can be even propagated at macroscopic spatial scales. Reversible large-scale superficial photopatterning and mechanical photo-actuation are efficiently achieved in azobenzene-containing glassy materials and liquid crystalline elastomers, respectively. This review covers several aspects related to the phenomenology and the applications of the light-driven macroscopic effects observed in these two classes of azomaterials, highlighting many of the possibilities they offer in different fields of science, like photonics, biology, surface engineering and robotics.

Keywords: azobenzene; azomaterials; azopolymers; liquid crystalline elastomers; mass migration; photo-actuation; surface patterning.

1 Introduction

Azobenzene-containing materials (or briefly azomaterials) are systems in which the azobenzene molecules are bonded or simply dispersed into another material. Many of the peculiar physical properties of this class of materials are attributed to the particular kinetics that the azobenzene molecules undergo when illuminated with UV and visible light. The absorption of photons with suitable energy produces cyclic structural transitions of the molecules between the *trans* and *cis* isomerization states. As the two isomers differ significantly in terms of structural conformation and volume, the photoisomerization of azobenzene is accompanied by a large motion at molecular scale. Such nanoscopic movement influences the surrounding chemical environment and can be highly amplified through the interaction of the photo-responsive units with a properly designed material system. In this respect, the motion of the photoisomerizing azobenzene molecules can be considered as the basic movement occurring at nanoscale in any azomaterial under light irradiation. Depending on the material architecture, the microscopic photo-induced movement can then eventually originate a series of macroscopic effects involving the collective rearrangement of the azobenzene molecules and the structural reconfiguration of the hosting material matrix at increasing spatial scales [1]. The technological implications of such multiscale phenomena are enormous, and azomaterials have been largely used to successfully design molecular compounds and material systems having specific light-tunable chemical, optical and mechanical properties. A huge amount of literature about the synthesis, the characterization and the applications of azobenzene-containing materials already exists. Each of these aspects is an active and rich field of research on its own, so all the perspectives involved cannot be exhaustively summarized together into a single concise review. Here, we shall try to provide a brief overview of the general scenario related to the many facets of azomaterials and their applications, focusing mainly the attention on the effects of macroscopic motions initiated by azobenzene photoisomerization.

The main focus of this review lies on the intriguing macroscopic phenomenon of the light-induced directional mass migration. Such phenomenon involves a mass transport at the free surfaces of thin amorphous azomaterial films (polymers, oligomers, molecular glasses), which

*Corresponding author: Antonio Ambrosio, Center for Nanoscale Systems, Harvard University, 9 Oxford Street, Cambridge, MA 02138, USA, e-mail: ambrosio@seas.harvard.edu
Stefano L. Oscurato, Marcella Salvatore and Pasqualino Maddalena: Physics Department "E. Pancini", University of Naples "Federico II", Complesso Universitario di Monte Sant'Angelo, Via Cintia, 80126 Naples, Italy

translates into topographic film modulation in the form of surface reliefs. Superficial structuration is obtained only in the illuminated areas of the film and is reversible and high directional, with a very peculiar sensitivity to the intensity distribution; to the polarization state; and, in some cases, even to the wavefront of the irradiating light beam. The vectorial dependence of the mass migration on the irradiating optical field components offers many possibilities for its use as a superficial photo-patterning technique. Here, the recent advances in this field are reviewed, together with several applications of the light-structured azomaterial surfaces in photonics, biology, surface engineering and lithography. In addition, the review includes also an overview of the macroscopic photo-actuation driven by structural *trans-cis* photo-switch of the azomolecules in azobenzene-containing liquid crystalline elastomers (azo-LCEs). The light-fueled motion of the azo-LCEs is the expression of a direct optical-to-mechanical energy conversion and represents a promising framework for emerging research fields aimed at the realization of light-driven artificial muscles, biomimetic soft-robotic locomotors and energy-harvesting devices.

2 The light-induced molecular motions of azobenzene

Due to the large range of possible applications derived from their inclusion into different material systems, azobenzene molecules and their photochemistry have been the subject of intensive studies. The detailed description of such aspects can be found in several reviews already existing in the literature [1–6] and is out of the scope of the present work. Here, however, the main features of the azobenzene molecules and their photo-induced dynamics are briefly discussed with the aim to provide an overview on the microscopic mechanisms underlying the macroscopic effects presented in the next sections and to highlight many application scenarios directly related to the use of azobenzene molecules as molecular photo-switches in azomaterials.

2.1 The azobenzene molecule

The chemical structure of the azobenzene molecules is characterized by two phenyl rings linked together through the azo bond (–N=N–). Azobenzene can exist either in the thermodynamically stable *trans* isomerization state or in the meta-stable *cis* isomerization state (Figure 1A). The *trans* isomer has a rigid and planar rod-like geometry, while in *cis*-azobenzene, the two phenyl rings form an angle of about 90° [7–13]. The azobenzene isomerization proceeds via rotation or inversion mechanisms around the azo-bond [5] and results in a reduction of the distance between the carbons in position 4 in the aromatic rings, which passes from 9.9 Å in the *trans* isomer to 5.5 Å in the *cis* isomer (Figure 1A). Besides generating volume variation [13–15] and large motion at molecular scale, the conformational switch between the *trans* and *cis* isomers of azobenzene is also accompanied by an increase of the molecular dipole moment (from $p_{\text{trans}} \approx 0$ to $p_{\text{cis}} \approx 3D$) [16, 17]. The *trans*-azobenzene absorption spectrum presents a broad absorption band associated to the pi-pi* transitions with peak at around 320 nm and a weak absorption band centered at about 450 nm originated by the n-pi* transitions. The latter absorption band becomes strengthened for the *cis*-azobenzene isomer [5, 18].

The most interesting feature of azobenzene molecules is the fact that the switch between the two isomeric forms can be initiated efficiently and repeatedly by the absorption of photons. The irradiation of an ensemble of azobenzene molecules lying in the energetically favored *trans*-state with UV light causes the switch of

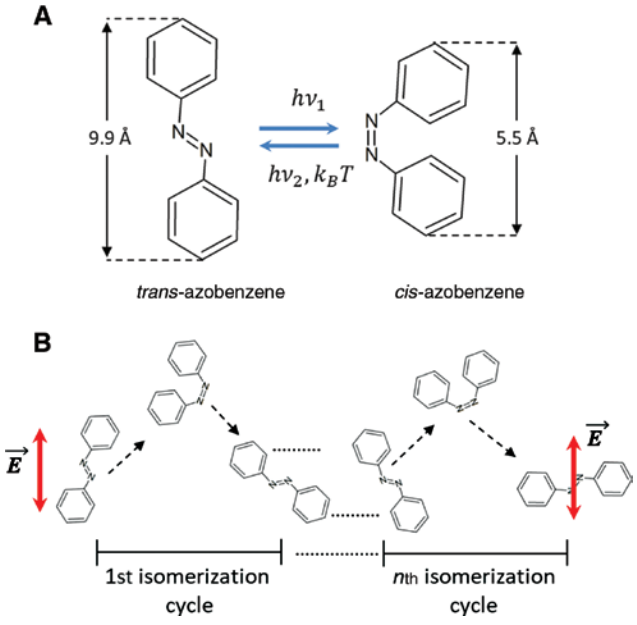

Figure 1: Molecular photo-dynamics of the azobenzene.
(A) The structural conformation of two isomers of azobenzene.
(B) Schematic illustration of the stochastic photo-alignment process of the azomolecules irradiated by linearly polarized light. The direction of molecular alignment is determined by the direction of the electric vector $\vec{E}$ in the irradiating optical field.

the molecular population to the *cis* isomerization state, which then can return back to the *trans* form either by thermal relaxation or by a new photo-reaction initiated by blue/green light (Figure 1A). The photo-induced reactions happen on time scales of a few picoseconds [19–21], while the thermal relaxation time from the *cis* to the *trans* state can range from fraction of milliseconds up to several days [3] depending on the molecular environment and on the actual chemical configuration of the phenyl rings, which can be eventually substituted with some functional groups. The substitution in azobenzene rings originates from a series of azobenzene-like compounds, generally referred to as azomolecules [22], which are characterized by the same structural *trans-cis* isomerization observed in the parent azobenzene molecules but eventually having different and tunable photophysical properties, like the position of absorption peak wavelength [22] or extremely long *cis*-state lifetimes [23–25].

In typical azomolecular systems, the absorption resonances initiating the *trans*-to-*cis* and the *cis*-to-*trans* isomerization transitions are broad and significantly overlapping. Then, even monochromatic photons (e.g. photons from a laser) of suitable energy (typically with wavelength in the range 400–550 nm) are able to efficiently activate both the photoisomerization reactions. As a consequence, an ensemble of continuously irradiated azomolecules undergoes repeated *trans-cis-trans* light-triggered isomerization cycles, which are able to initiate another light-driven molecular scale motion in azobenzene-containing systems. Such microscopic movement involves the stochastic photo-reorientation of the azounits irradiated with linearly polarized light [26, 27]. The photo-reorientation of the azomolecules is derived from the enhanced absorption probability, and hence from the more efficient isomerization dynamics, for the molecules excited with light polarized along the direction of their molecular transition dipole, this being oriented along the molecular main axis of the *trans* isomer. The dynamics of the molecular reorientation process is schematized in Figure 1B. As the orientation of the molecular axis of a *trans*-azomolecule varies randomly in each photoisomerization cycle, after many of them, the excited azounit can become stochastically oriented in the direction orthogonal to the light polarization direction. The photoinduced dynamics of such reoriented azomolecule stops as it does not absorb photons efficiently anymore, remaining oriented at 90° in respect to the light polarization direction even if the light irradiation continues. Such polarization-induced "invisibility" to new polarized photons of the reoriented azocromophores is commonly referred to as orientational hole-burning and causes a lowering of the population of *trans* isomers oriented in the polarization direction, together with a concomitant enrichment of the population of *trans* molecules oriented in the direction orthogonal to the polarization plane. Naturally, the molecular reorientation is reversible and reconfigurable. A new alignment can be realized in any desired direction simply by a rotation of the irradiating linear polarization direction. Eventually, even the initial isotropic molecular distribution can be easily restored by the irradiation of circularly polarized or non-polarized light [28].

2.2 Photo-switch in azomaterials

The geometrical reconfiguration of the azomolecules and their reorientation under light irradiation directly affect the configuration and the functionality of the molecular environment in which they are incorporated, behaving essentially as controllable and reversible photo-switches. For example, the conformational molecular rearrangement associated with the photoisomerization reaction able to transform the mesogenic *trans* isomer into the non-mesogenic *cis* isomer has been largely used to efficiently trigger phase transitions in azobenzene-containing liquid crystalline material systems [29–32]. The *trans-cis* structural photo-switch has recently been employed in several biological applications [33–35]. For example, the isomerizing azomolecules have been used to photo-activate molecular mechanisms able to control on demand the aperture and the closure of the channels through the cellular membranes for controlled ion transport [36–38] or the three-dimensional (3D) structure of proteins [39]. The variation in the molecular dipole moment occurring in the isomerization photo-switch has been also successfully exploited as a light-controllable switch of compound solubility [40] and for the reversible tailoring of the wetting properties of solid azobenzene-functionalized surfaces [41–48]. Even the directional and controllable light-driven displacement of liquid droplets has been demonstrated [49]. Furthermore, recent studies used photo-switchable azobenzene-containing surfactants to control the movement of particles at the liquid/solid interface through light-driven diffusioosmosis [50–52]. The photo-orientation effect of the azomolecules gives origin to strong birefringence, dichroism and non-linear optical effects [1, 53–58]. Based on these properties, azobenzene-containing materials have been proposed as a platform for reversible data storage and holographic recording [28, 29, 59–61]. The photo-orientation is also able to control the direction of ordering in liquid crystalline matrices, doped with cyclically isomerizing and re-orientable azocromophores

[62–65]. Furthermore, the in-plane photo-reorientation of molecular azobenzene monolayers deposited onto a substrate has been used as aligning layer in liquid crystal (LC) cells, allowing the realization of spatially structured alignment geometries not easily accessible with conventional mechanical rubbing [66, 67].

3 The directional light-induced mass migration in azomaterials

In 1995, Natansohn and Rochon [68] and, independently, Kim et al. [69] reported for the first time about the large-scale periodic modulations of the free surface of a thin amorphous azobenzene-containing polymer film irradiated with the sinusoidal intensity light pattern produced by the interference of two mutually coherent p-polarized laser beams (Figure 2A). The resulting sinusoidal superficial texture, now commonly referred to as surface relief gratings (SRGs), presented an amplitude modulation of several hundreds of nanometers and a groove pitch matching the periodicity of the illuminating interference pattern (Figure 2B–C), hence showing an exact replica of the irradiated light intensity pattern in the form of surface modulations.

The light-induced superficial texturing was observed to occur at very low irradiation intensities, discarding any explanation of the phenomenon in terms of the ablative or destructive processes [70, 71]. On the contrary, topographic modulation was immediately understood as the result of an actual material movement, induced efficiently by the irradiating light even for temperatures significantly lower than the glass transition temperature T_G of the employed amorphous azomaterial [68, 72]. The non-destructive nature of the phenomenon emerged immediately also from the almost complete volume conservation in the written area [73] and from the possibility of erasing (and then eventually rewriting) the inscribed superficial textures either by rising the temperature of the film above T_G or by irradiating the structured film with circularly polarized or non-polarized uniform light distributions [74–76].

Since the first fundamental discoveries, a large amount of research has been oriented toward the study of this intriguing light-induced phenomenon, with great multidisciplinary interest in both theoretical and applied research fields. This can be immediately understood by thinking of the phenomenon as the macroscopic manifestation of a unique complex microscopic light-matter interaction, whose actual underlying mechanism is still debated in the scientific community. Moreover, and more importantly, the non-destructive reversible process of the light-driven mass migration offers countless possibilities in several applied and technological areas. The high scientific impact of the subject is also witnessed by the high number of reviews already available in literature, which cover many of the aspects of the light-driven superficial structuration and several its possible applications [1, 3, 75, 77–80].

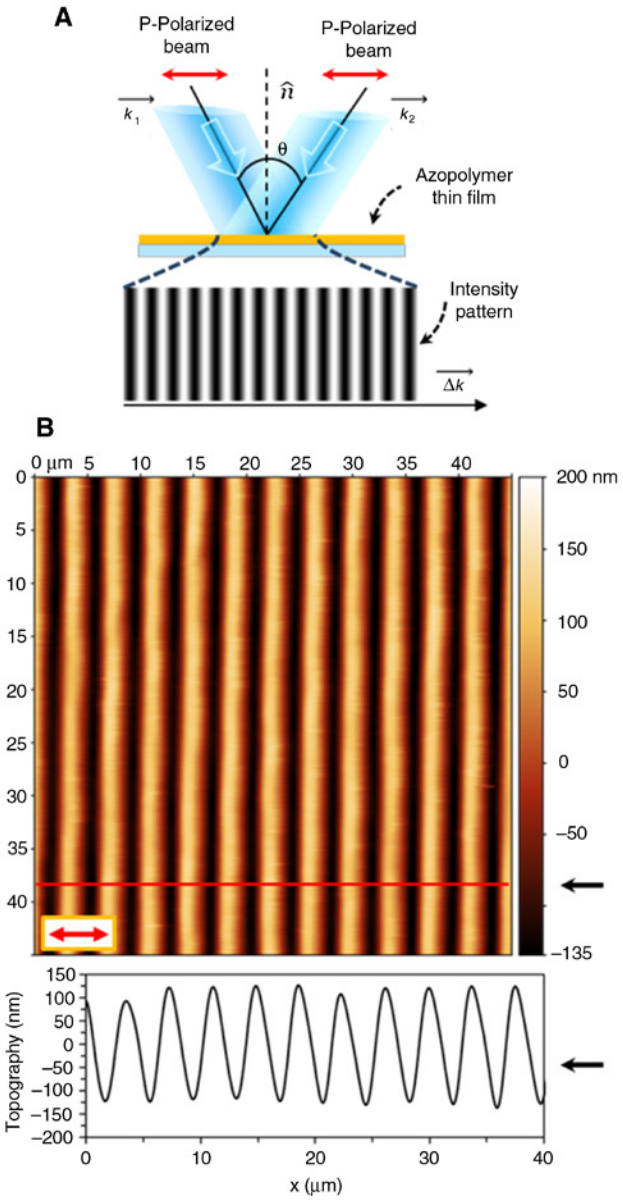

Figure 2: The SRGs induced onto an azopolymer film by the irradiation of an intensity pattern produced by two interfering p-polarized beams. (A) Schematic representation of the typical illumination configuration used for the inscription of SRGs. (B) AFM image and amplitude topographic profile (traced along the red line) of the SRGs in (A). The red arrow indicates the polarization direction of the two interfering beams.

The next sections of the present chapter include an overview on the well-established general rules governing the light-induced mass migration and the resulting superficial structuration of the azomaterial films. The dependence of the surface reliefs on the intensity; on the polarization; and, in some cases, also on the wavefront distributions of the irradiating light is described, providing a solid global picture of the phenomena involved in the large number of applications presented later in the chapter. Finally, the differences in the behavior of the material transport observed in some cases for different material systems and/or illumination configurations are also evidenced, with the aim of triggering further research in both fundamental and technological fields related to this intriguing light-matter interaction.

3.1 The phenomenology

3.1.1 Material design strategies

From the perspective of material design, the prerogatives for an efficient light-induced mass transport are the efficient *trans-cis-trans* cyclic photoisomerization of the azomolecules and the inclusion of these molecules in amorphous material matrices. A well-defined chemical interaction between the hosting material and the photo-active azounits has been demonstrated to increase the efficiency of the material transport in respect to the simple blended azomaterials [81, 82], and several binding strategies (including covalent attachment [1, 83], ionic interactions [84, 85] and supramolecular interactions as hydrogen and halogen bonds [86–89]) have been exploited to design light-responsive azomaterials showing efficient mass migration. The most commonly used material platform involves the use of amorphous polymers (simply referred to as azopolymers) as inert hosting matrix. Also, other materials lying in the glassy state, like molecular glasses [90, 91], oligomers [92, 93] and dendrimers [94–96], have turned out to give rise to efficient light-driven material transport, while only smaller effects in terms of surface modulation have been found in liquid crystalline azopolymers [97–100].

3.1.2 Intensity and polarization dependence

The fingerprint of the light-induced mass migration phenomenon in azomaterials is the peculiar sensitivity of the material transport to the intensity distribution and the polarization state of the irradiating light field. Under the irradiation of polarized light, the material motion turns out to be highly directional, with the polarization direction constituting a preferential direction along which the material transport mainly occurs.

The general aspects of the intensity/polarization-dependent directional material motion occurring in the presence of a spatially structured illumination pattern can be easily understood from the surface reliefs generated in the irradiation of an azopolymer film with focused linearly and circularly polarized Gaussian beams. In the case of linear polarization, the surface structuration reflects a polarization-driven anisotropic material displacement. The surface relief is indeed constituted by a depression appearing in the region of the laser focal spot, with two lobes raised above the film average quote and oriented along the direction of the linear light polarization (Figure 3A). When the Gaussian beam is circularly polarized, no preferential direction exists for the material motion, as the optical electric field in this polarization configuration is, on average, isotropically oriented in all the directions of the film plane. In this situation, the two overhead lobes obtained in the case of linear polarization are substituted by a symmetric annular relief (Figure 3B) [101, 103]. As a Gaussian beam has an isotropic intensity gradient in the focal plane, the surface reliefs obtained in this illumination condition allow to further characterize the direction of the mass migration in respect to the intensity distribution of illuminating light field. Indeed, the appearance of the hole in correspondence with the intensity maximum of the focal spot reflects another general feature of the directional material displacement, actually proceeding from high- toward low-intensity regions of a structured irradiating light pattern.

The directional mass transport can occur also under uniform-intensity distributions whenever the azomaterial surface presents a structural discontinuity able to break the in-plane isotropy of the (typically spin-coated) homogeneous flat films. A simple example of such anisotropic azopolymer surface is presented in Figure 3C, where a series of scratches are mechanically practiced in orthogonal directions over a flat azomaterial film [102, 104]. The irradiation of a single collimated and linearly polarized beam produces a selective filling only of the canals oriented perpendicularly to the linear polarization direction (Figure 3D–F), highlighting again a highly directional azomaterial displacement in the light polarization direction. This observation reveals an azomaterial motion behaving similarly to a light-fueled directional liquid flow, which is able to reconfigure the pre-patterned azopolymer surface analogously to the isotropic thermally induced material fluidization used in the lithographic technique named self-perfection by liquefaction (SPEL) [105, 106]. The

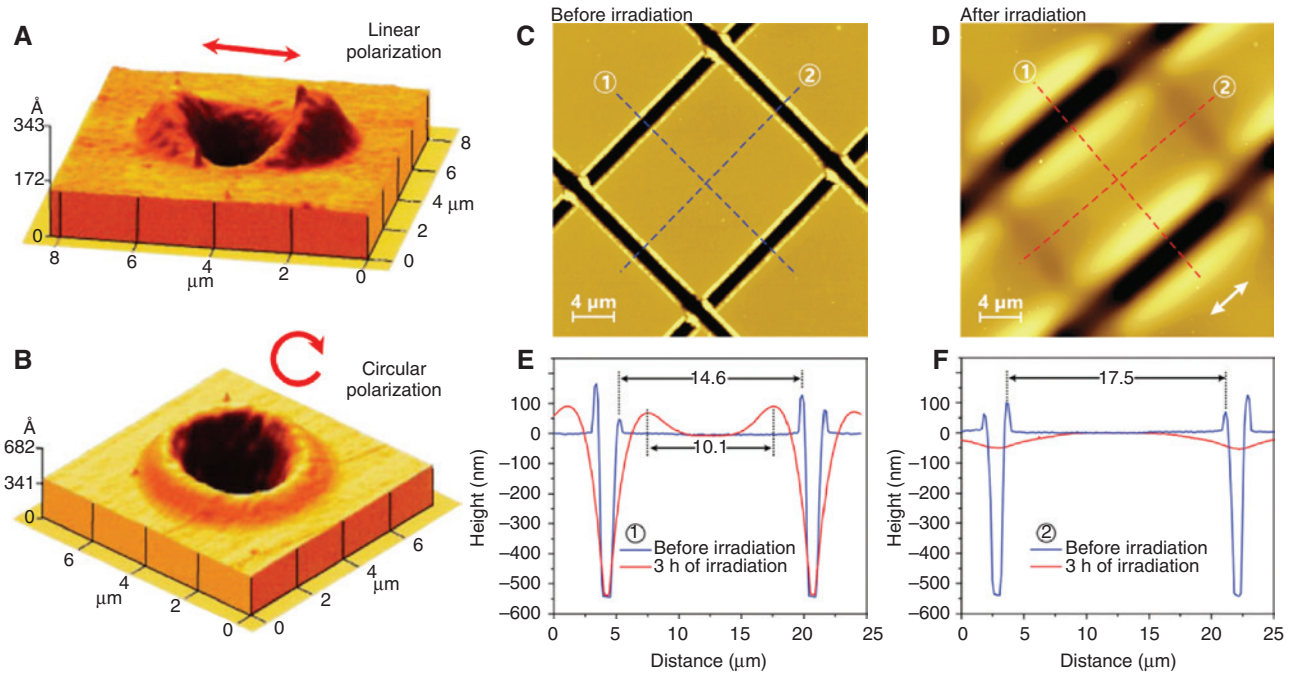

Figure 3: Polarization-dependent directional mass transport in azopolymers.
Surface reliefs resulting from linearly (A) and circularly (B) focused Gaussian beams. (A–B) Adapted from Ref. [101] with permission from AIP Publishing. (C–F) Polarization-dependent selective filling of scratches practiced in orthogonal directions over an azopolymer surface. Reproduced from Ref. [102] with permission from the Royal Society of Chemistry.

phenomenological analogy with SPEL has nevertheless led to the introduction of the concept of directional photofluidization (DPF) [79, 104] to describe the anisotropic light-driven mass migration phenomenon in azomaterials. However, the eventual light-induced liquefaction of the azomaterials has not been unambiguously demonstrated in the literature, with the actual viscoelastic and mechanical properties of the azomaterials under irradiation being still subject of intense investigation [71, 107–115] and debates in the scientific azo-community [116].

From the described intensity/polarization dependence, it is clear that, when the irradiating light field has a preferential direction in the spatially modulated intensity pattern (as in the case of the sinusoidal intensity distribution produced in the interference of two parallel polarized laser beams), the direction of the intensity gradient should match the direction of the linear light polarization in order to achieve a highly efficient surface structuration. Indeed, differently from the case of p-polarized beams, only small surface modulation is observed upon the irradiation of an intensity interference pattern obtained by two s-polarized interfering beams, where the intensity gradient and the polarization direction are mutually orthogonal.

Such behavior has been confirmed several times by polarization-dependent experiments involving the monitoring of the growing dynamics of SRGs inscribed with intensity patterns generated by two interfering beams in different polarization configurations [72, 81]. More recently, these kinds of polarization-dependent studies have been accurately performed by direct *in-situ* analysis [102, 117–123] conducted through microscopic setups having the powerful ability to monitor in real time both the evolution of the topographic surface structuration and the irradiating light fields (Figure 4A–F). Also the relative π-phase shift between the maxima in the intensity patterns and the topography maxima in SRGs resulting from a material migration from illuminated to dark areas of the spatially structured interference intensity pattern has been unambiguously observed with such setups [102, 117–123]. Similar polarization-dependent experiments have highlighted a high efficiency for the SRGs formation even under pure polarization interference patterns, in which the intensity distribution is uniform but the orientation of the electric field vector is spatially modulated over the sample (Figure 4G–I) and the material motion is driven by a pure polarization gradient [83, 85, 114, 120–122, 124–126].

In some cases, however, the polarization-dependent structuration of flat azomaterial surfaces is obtained even under both uniform intensity and polarization light distributions. Indeed, also the irradiation of a single collimated beam can induce periodic textures over the illuminated

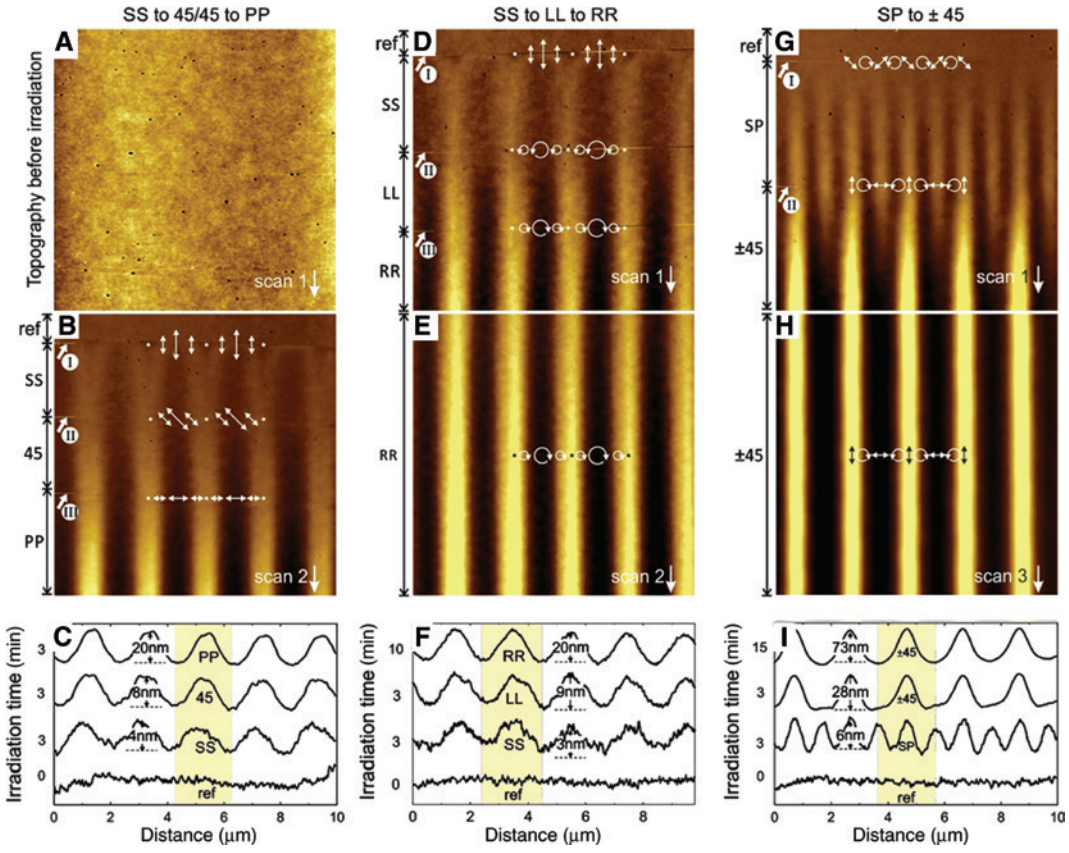

Figure 4: SRGs induced by different polarization combination and recorded by real-time *in situ* AFM.
The vertical direction in the AFM images corresponds to a time axis. (A) Topography before the irradiation. (B) Time evolution of the film topography obtained by switching the polarization of the two interfering beams from S-S to 45°-45° to P-P at the positions indicated by the Roman numbers. (D–E) Same as before for polarization switches from S-S, to left circular (L-L) and to right-circular (R-R). (G–H) Same as before for the pure polarization interference patterns produced by S-P and +45°/ – 45° polarized beams. The topographic profiles relative to each polarization configuration are shown in panels (C, F, I). Reprinted from [121] with permission from Springer, copyright 2013.

azomaterial film [127–145]. Linearly polarized beams produce unidimensional (1D) periodic grooves, whose orientation depends on the light polarization direction (Figure 5A–F). The irradiation of a circularly polarized or non-polarized light beam induces instead protrusions arranged in hexagonal arrays (Figure 5G–I). The structural features of such spontaneous superficial patterning of the azopolymer films share several aspects of the laser-induced periodic superficial structuring (LIPSS) occurring at the surface of many solids when irradiated with intense pulsed laser beams [146–148]. However, differently from such thermally induced phenomenon involving material ablation, the spontaneous structuring of the azomaterial film occurs efficiently also for continuous low intensity regimes and has been recognized as resulting again from the mass migration phenomenon [131, 133, 140]. Because of the phenomenological and structural analogies with the large-scale sinusoidal superficial texture of the SRGs, the periodic large-scale superficial modulations obtained with a single irradiating beam are typically referred to as spontaneous surface relief gratings (SSRGs).

3.1.3 The effective wavefront sensitivity

The appearance of spiral-shaped surface reliefs [149, 150] under the irradiation of an azopolymer film with focused Laguerre-Gauss (L-G) beams (Figure 6A) has allowed the discovery of an effective wavefront sensitivity of the light-induced mass migration, which, in particular illumination configurations, can be added to the already mentioned dependence of the phenomenon on the intensity and polarization distributions of the illuminating optical field.

In these experiments [149, 150], the inscribed spiral surface reliefs showed a direct dependence on the beam parameter (the vortex topological charge, q), which characterizes the properties of the helically shaped wavefront of the L-G beams [151–154]. In particular, larger values

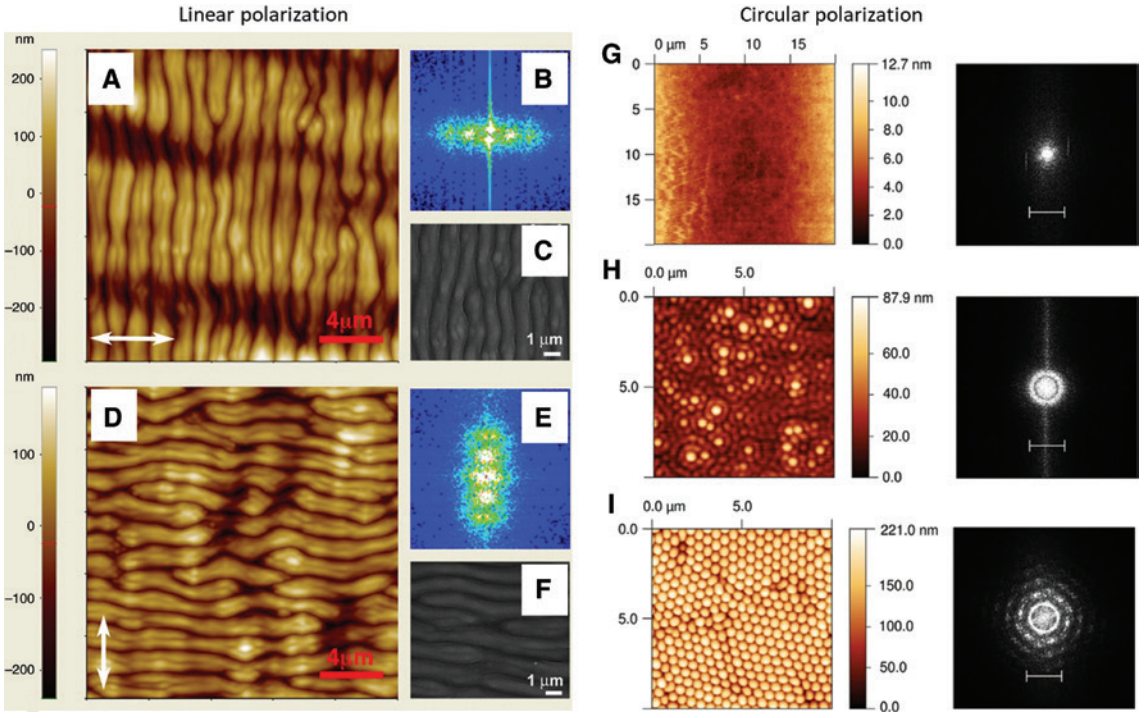

Figure 5: SSRGs generated by linearly and circularly polarized single beams.
AFM images (A and D), 2D Fourier transform (B and E) and SEM images (C and F) of the SSRGs induced by a collimated beam, linearly polarized along the two orthogonal directions indicated by the white arrows. (A–F) reproduced from Ref. [138] with permission from AIP Publishing. (G–I) AFM images and their relative Fourier transforms of the SSRGs at different exposure times obtained with a circularly polarized beam. Adapted from Ref. [143] with permission from Elsevier.

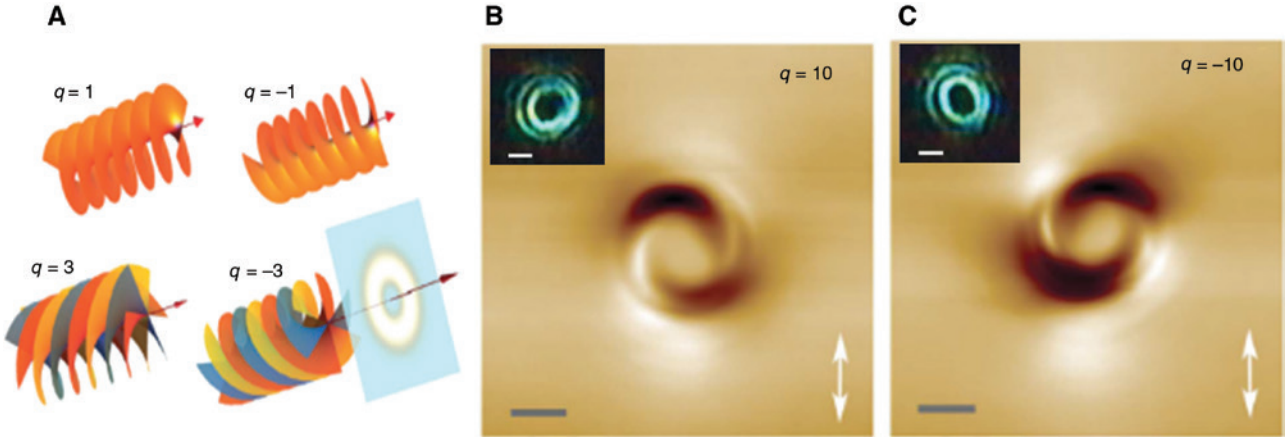

Figure 6: The spiral surface reliefs and the wavefront sensitivity.
(A) Illustration of the helically shaped wavefronts (dependent on the vortex topological charge q) and doughnut-shaped intensity profiles of optical vortex beams. (B) AFM images of the spiral surface reliefs generated by a focused, linearly polarized, $q = 10$ vortex beam (polarization direction indicated by white arrows). The inset shows the optical image of the irradiating light intensity pattern. (C) Same as in (B) for the spiral surface relief generated by a focused $q = -10$ vortex beam. Scale bars: 1 μm. Adapted with permission from Ref. [149], copyright 2012, Springer Nature.

of $|q|$ translate into larger spiral diameters, while the inversion in the sign of the topological charge produces an inversion in the handedness of the inscribed spiral reliefs (Figure 6B–C). As information about such helicity is contained only in the beam wavefront and not in the intensity and polarization distributions of the doughnut-shaped irradiating L-G beam, the natural hypothesis for the interpretation of the observed spiral mass transport

is that light-induced mass migration is sensitive to the wavefront of the irradiating light beam in this particular illumination condition. Even if the spiral surface reliefs are, until now, the only experimental situation where such wavefront sensitivity has been clearly highlighted, the inclusion of this degree of freedom can enlarge significantly the possibilities offered by the light-driven structuration of the surface of azopolymer films for applications in nano-lithography.

3.1.4 A complex light-matter interaction

The rationalization of the huge phenomenology associated to the azomaterial light-induced mass migration in a complete theoretical framework is still an open question. While the photoisomerization of the azomolecules is thought as absolutely necessary in order to observe any significant superficial structuration, the physical link between this microscopic movement and the observed macroscopic azomaterial displacement has not been unambiguously recognized yet. Several different theoretical models have been proposed over the years with the aim of elucidating this intriguing light-matter interaction. One of the general requirements, common to several hypothesized microscopic mechanisms, is the presence of optical gradients in the intensity and/or in the polarization of the illuminating light able to induce some variation in the physical properties of the material as a consequence of spatially dependent photoisomerization dynamics of the azounits. Effects including a gradient in the pressure forces inside the material [155, 156], the electric interactions among the molecular dipoles of the re-aligned azos [75], the mechanical stress induced by the azo photoreorientation [157, 158], the motion driven by gradients in the electromagnetic forces [103, 159–161] and the anisotropic diffusion or random-walk [150, 162–164] of the azomolecules have been proposed as driving microscopic mechanisms of the phenomenon. Recently, also the phase separation among the *trans*-rich and the *cis*-rich microdomains, eventually induced in the azomaterial film by the irradiating light, has been hypothesized as a possible fundamental microscopic driving mechanism [140]. However, none of the proposed models were able to effectively describe all the experimental observations, their validity being typically limited to specific material systems or to specific illumination conditions.

In the literature, also reports about few situations where the mass migration phenomenon gives rise to a different phenomenology can be found. For example, in some conditions, the interfering beams in s-s polarization configuration can drive the efficient formation of SRGs, whose amplitude can depend on material characteristics (e.g. material molecular mass) [165, 166] or on the presence of an assisting beam recycling the orientational population of the isomerizing azomolecules during the inscription process [117, 161, 167]. Even an inversion in the direction of the material displacement has been observed in the SRGs inscribed in certain amorphous [123, 168] and in liquid crystalline azopolymers [78, 97, 100, 169, 170], where the topographic maxima arise in correspondence with the maxima in the light intensity pattern. A similar inversion in the mass migration direction has also been found in experiments where a focused laser beam is scanned across a glassy azopolymer surface [49, 145], with a polarization direction chosen to be parallel to the scanning direction (Figure 7A–B). Also, the direction of the light-induced deformation observed in isolated micropillars under uniform linear light polarization (Figure 7E–G) has been found to depend on the nature of the employed azomaterial [168]. Furthermore, “conch-shaped” surface

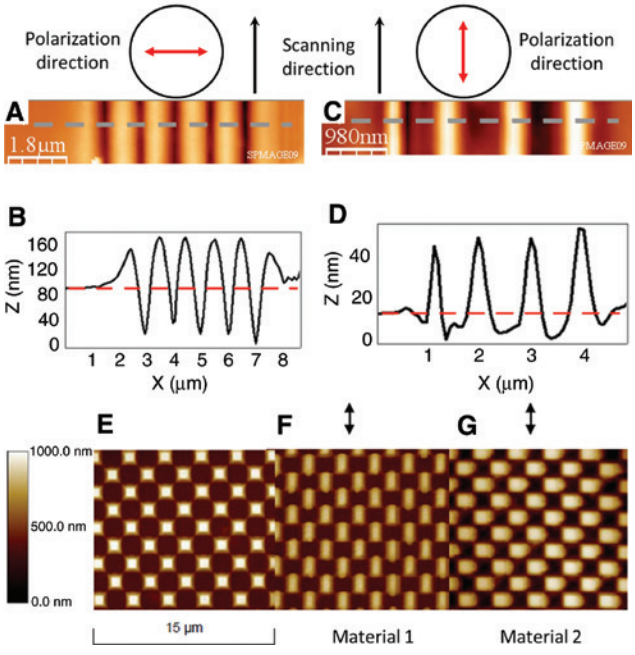

Figure 7: Dependence of the material displacement direction on illumination conditions and chemical nature of azomaterial systems. AFM images and topographic profiles of the surface reliefs generated onto an azopolymer by a scanning focused laser beam linearly polarized in the direction orthogonal (A–B) and parallel (C–D) to the fast scanning direction. Adapted from Ref. [73] with permission from AIP Publishing. (E) A pristine array of square micro-posts (E) deformed in the direction parallel (F) or orthogonal (G) to the linear light polarization depending on the chemical nature of the employed azomaterial. Reproduced with permission from Ref. [168].

reliefs, instead of spirals, have been obtained on the surface of an azopolymer illuminated by a focused L-G beam in intense irradiation conditions, as reported in Ref. [171].

The observed huge phenomenology is certainly attributed to the simultaneous coexistence of different microscopic physical processes driving the mass migration under light irradiation, whose relative efficiency has been hypothesized as dependent on material chemistry [123, 157] and on illumination parameters as the light intensity level or the complex spatial distribution of the optical electromagnetic fields inside the azomaterial film [103, 117–119, 161, 172–177]. However, while unveiling the nature of these microscopic effects is of great interest from the perspective of the rationalization of complex light-matter interactions at a fundamental level, in all the practical applications aimed to use light-induced surface structuration of azomaterials, comprehension of the exact and general microscopic mechanism can be effectively overcome by phenomenological descriptions of the phenomenon. With a such approach, the surface modulation can be qualitatively, but precisely, predicted for each particular azomaterial system of interest on the basis of the knowledge of the characteristic empirical response to simple illumination configurations (e.g. focused polarized beams) and the actual vectorial distribution of the optical field inside the irradiated azomaterial film.

A promising powerful phenomenological model able to reproduce and qualitatively predict almost all the experimental observations is given in Refs. [149, 150]. In these works, the azopolymer surface structuration is described as related to the optical field components of the irradiating light by the following relation:

$$\begin{aligned}\Delta h(x,y) = {} & (c_1+c_2)[\partial_x^2|E_x|^2+\partial_y^2|E_y|^2]+c_1(\partial_x^2|E_y|^2+\partial_y^2|E_x|^2)\\ & +c_2\partial_x\partial_y(E_x^*E_y+E_y^*E_x)+c_3(\partial_x^2|E_z|^2+\partial_y^2|E_z|^2)\\ & +c_B[\partial_x Re(E_z^*E_x)+\partial_y Re(E_z^*E_y)]\end{aligned}$$

Here, $\Delta h(x, y)$ is the variation of the surface amplitude describing the surface relief across the polymer film; $\boldsymbol{E}=(E_x, E_y, E_z)$ is the optical electric field of the irradiating light; and c_1, c_2, c_3 and c_B are phenomenological constants characteristic of the actual employed azomaterial. The phenomenological relation includes terms (proportional to c_1, c_2, c_3) depending explicitly on the intensity distribution and its gradient, whose sign and relative strength can be empirically adjusted in order to reproduce most of the phenomenology observed in typical illumination schemes (SRGs and focused beams) [149]. Moreover, the last term in the phenomenological expression, proportional to the constant c_B, describes a surface-mediated interference between longitudinal and lateral field components of the irradiating beam. Such a term is identically vanishing in almost all the simple illumination schemes but is the one responsible for the spiral mass transport observed in the irradiation of focused L-G beams [149] (Figure 8) and hence for the effective wavefront sensitivity observed experimentally in this illumination configuration. Such surface-mediated interference term has been found to play a main role also in the explanation of the light-induced directional mass migration phenomenology observed in the reconfiguration of sharp edges (scratches and isolated microvolumes) of prestructured azomaterial surfaces under uniform illumination distributions. In this illumination configuration, both intensity and polarization gradients

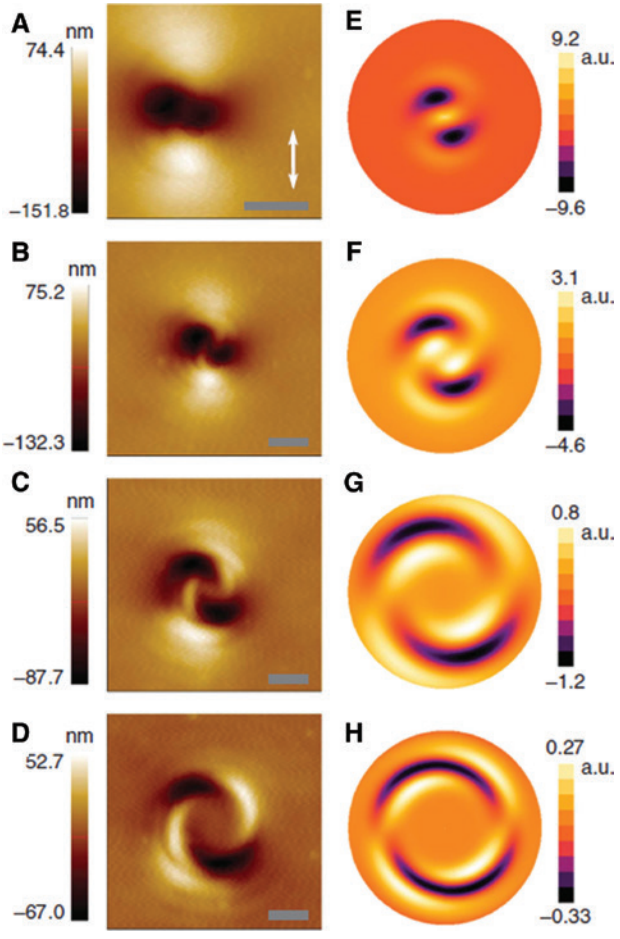

Figure 8: The spiral surface reliefs predicted by the phenomenological model proposed in Ref. [149].
(A–D) AFM images and (E–H) relative predicted spiral surface reliefs for different vortex topological charges. The light polarization direction is indicated by the white arrow. Scale bars in panels (A–D): 900 nm. Reprinted with permission from Ref. [149], copyright 2012, Springer Nature.

in the light field are identically vanishing and the only non-vanishing contributions to the light-induced mass current flow causing the surface reconfiguration comes from the coupling of the homogenous optical field with the discontinuities of the pristine prestructured surface. As described in Ref. [178], this surface-initiated material motion is again well-described by the term proportional to the constant c_B in the phenomenological model.

3.2 The photo-patterned azomaterial surfaces and their applications

The general rules governing the phenomenology of the macroscopic light-induced surface structuration of amorphous azomaterials were soon understood, and the literature contains a large number of examples where the light-patterned azomaterial films are concretely used for fundamental and technologically oriented studies. Applications range from the high-resolution photochemical imaging of optical fields, in which the intensity and polarization sensitivity of the light-induced surface reliefs are directly used to extract the information about complex optical fields, to large-scale surface photo-patterning. In relation to this last aspect, the next sections of the present chapter cover several situations in which the large-scale photo-structuration of azopolymer surfaces is employed to modify different structural properties and functionalities of the azomaterial films themselves or to structure the surface of other materials. In particular, the possibilities in terms of complex and controllable photo-patterning offered by the SRGs and the light-induced reconfiguration of azopolymer isolated microstructures and microvolumes are discussed together with their possible applications in wettability, biology, photonics and photolithography.

3.2.1 Photochemical imaging of optical fields

As the light-induced mass migration behavior depends on the illumination parameters in a vectorial manner, the surface reliefs in azopolymers can be used to map the vectorial distributions of unknown optical fields [179]. A first example of such kind of application is represented already by the spiral-shaped surface reliefs described above. In particular, it is legitimate to suppose that, whenever a spiral surface relief appears on an azopolymer surface, the irradiating beam is probably endowed with an optical vortex. In this scheme, the peculiar spiral-shaped surface reliefs become a fingerprint impressed into the azopolymer surface of a beam endowed of an optical vortex.

One of the key features making the light-induced surface reliefs attractive for applications in the photochemical imaging of optical field is the possibility to reach spatial resolutions far beyond the ones achievable with diffraction-limited far-field imaging techniques. Such high spatial resolution is, moreover, achieved by using a simple AFM analysis, in which the reconstruction of the high-resolution information about the optical fields comes directly from the topographic characterization of the irradiated azomaterial film, without the necessity of using powerful but sophisticated near-field imaging techniques (e.g. near-field optical microscopy, NSOM [180–184]).

This optical-to-topographical information conversion was revealed to be a powerful tool for the imaging of polarization-dependent near-field optical distributions in the proximity of metal nano-structures. An example of such sub-diffraction resolution imaging approach relies on the photochemical imaging of the local field enhancement obtained in proximity of an illuminated metallic-coated nanometric tip. The light field confined at subwavelength scales near the tip produces a local nanometric protrusion onto an exposed azopolymer film, whose structure is directly dependent on the tip geometry and polarization state of the irradiated light [177, 185]. Such nanometric surface reliefs have also been suggested as usable for lithographic patterning of the azopolymer films at subwavelength spatial resolution [186]. In other experiments, the surface reliefs have been used to image the plasmonic field produced by metallic nanostructures. For such applications, an azopolymer film is typically spin-coated onto an array of metallic nanostructures, which were fabricated onto a substrate by means of high-resolution standard lithographic techniques. The optical near-field in proximity to the nanostructure generates surface reliefs whose configuration is strongly correlated with the intensity pattern of the plasmonic field predicted from theoretical models. For example, Bachelot et al. found a qualitative agreement of the surface reliefs experimentally observed in proximity of silver nanodisks (Figure 9A–F) and bowtie nanoantennas (Figure 9G–I) with the negative images of the intensity distribution predicted by theoretical calculation on the plasmonic fields in different polarization configurations [164, 187, 188]. These results are simply interpreted assuming the typical material motion in the presence of intensity gradients along the direction of light polarization. In similar experimental conditions, also the interference of surface plasmons has been successfully recorded in an azopolymer film [189–191].

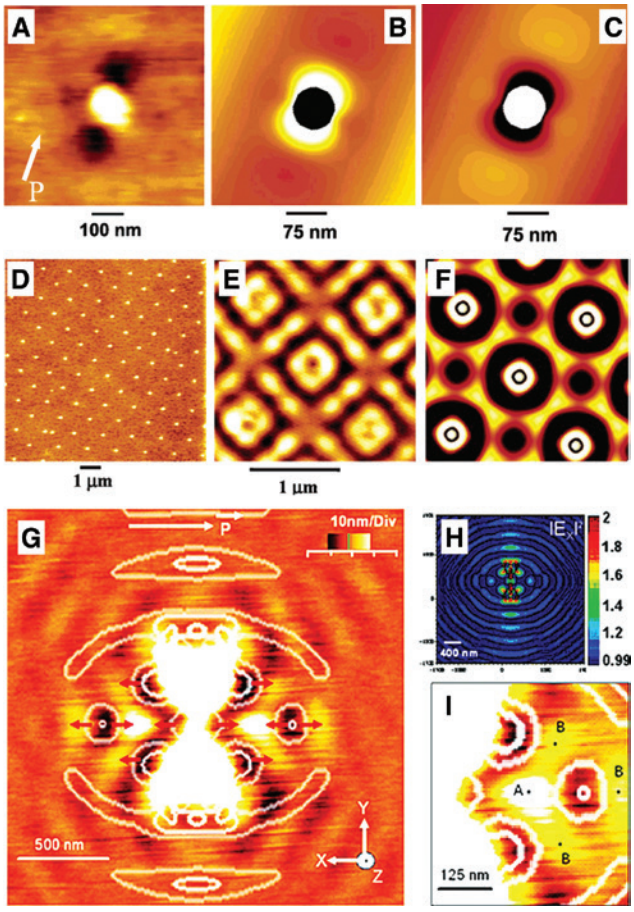

Figure 9: Photochemical imaging of optical fields in the form of surface reliefs.
(A) Topographic image and (B) theoretical calculation of the near field distribution generated by a linearly polarized beam (white arrow) around an azopolymer-coated silver nanoparticle. (E) Surface reliefs generated by the irradiation of an array of azopolymer-coated silver nanoparticles (D) with circular polarization. Panels (C) and (F) show the negative images of the predicted intensity patterns in the two polarization configurations. Adapted with permission from Ref. [187], copyright 2005, American Chemical Society. (G) and (I) AFM images of the topographic modulation of an azopolymer film covering a bowtie nanoantenna, irradiated with a x-polarized beam. The predicted intensity profile along the x direction is shown in panel (H). Reprinted with permission from Ref. [188], copyright 2008, American Chemical Society.

3.2.2 Surface relief gratings as large-scale periodic superficial textures

One of the key features making the SRGs attractive as a large-scale, easy and flexible technique for the micro-nanofabrication of textured surfaces is the possibility of tuning few irradiation parameters affecting the behavior of the material transport to precisely control the final surface topography. Indeed, at fixed irradiation wavelength, the periodicity Λ of the SRGs in a selected direction over the surface is determined only by the angle θ between the two interfering beams according to Bragg's relation $\Lambda = 2/[\sin(\theta/2)]$, while the amplitude of the grooves, inscribed in any chosen polarization configuration, depends on the light fluence. Periodic surface reliefs, extended over areas of a few square centimeters, with amplitudes up to 1 μm [85] and periods ranging from hundreds of nanometers to several micrometers, can be easily obtained in very simple and cost-effective experimental conditions, typically constituted by a single irradiation step of azomaterial film with two interfering light beams.

Besides the 1D SRGs, more complex bidimensional surface reliefs arranged in tetragonal, hexagonal or even more complex configurations can be easily obtained by

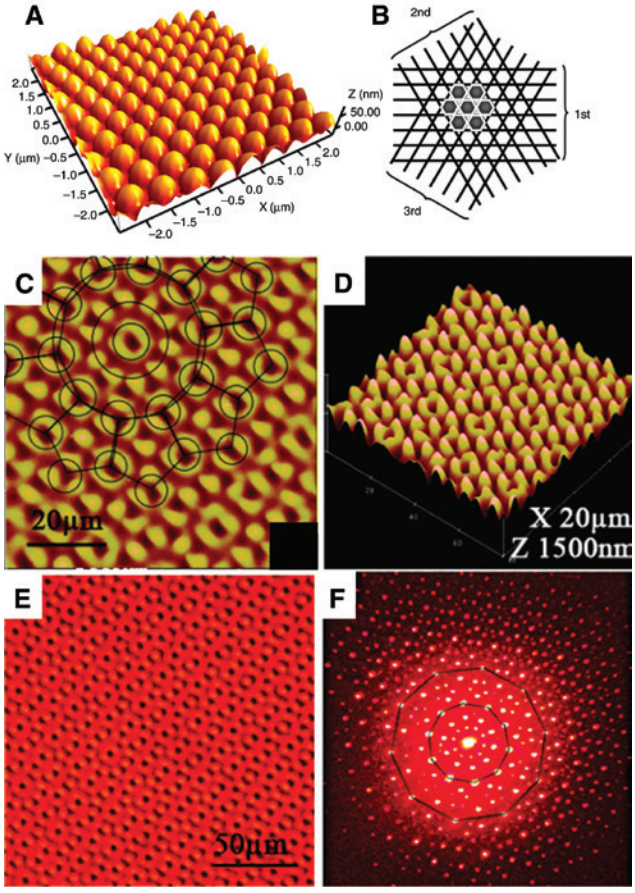

Figure 10: Complex SRGs from multi-step irradiation.
(A) AFM image of the SRGs generated by rotating the azopolymers by 120° in three subsequent irradiation steps (B). (A–B) Reproduced with permission from Ref. [193], copyright 2008, The Japan Society of Applied Physics. (C–D) Topographic images of quasi-crystal superficial structure resulting from five illumination steps, each at $\pi/5$ sample rotation angle. Optical image (E) and He-Ne diffraction pattern (F) of the 10-fold quasicrystal SRGs. (C–F) Adapted with permission from Ref. [91], copyright 2008, American Chemical Society.

two or multiple successive inscription steps of 1D SRGs in different directions over the film [83, 192, 193]. An example of the hexagonal grating induced in a three-step illumination procedure in which the azomaterial film is rotated by 120° at each step is shown in Figure 10A–B, while a quasicrystal pattern [91, 194] with 10-fold symmetry resulting from five subsequent irradiation steps (each for a rotation angle $\pi/5$) is shown in Figure 10C–F. Other complex and periodic superficial textures can be achieved also in experiments where irradiation is accomplished with three or more interfering beams [75, 195–197].

Also the surface structuration obtained in the case of the SSRGs can be of particular interest for cost-effective, all optically driven surface structuration. The periodicity of the SSRGs is controlled by the wavelength of the irradiating light [131, 141] and by the incidence angle of the collimated beam [130], offering a possible deterministic tuning of the inscribed surface modulation. Even if the number of accessible superficial textures of SSRGs is lower when compared to the SRGs, these being limited to parallel groves or hexagonal arrays, the large-scale tunable superficial textures of the SSRGs in the simplest conceivable illumination configuration constituted by a simple single irradiation step with a collimated light beam.

Regardless of the degree of geometrical complexity achievable onto the surface, the texture of the azomaterial film can be erased, and eventually rewritten, at will, taking advantage of the reversible nature of the photo-driven phenomenon of the mass transport [76, 198]. Particularly relevant for the realization of reversible all-optical patterned surfaces is the possibility to remove the inscribed superficial structuration by irradiating the film with circularly polarized or unpolarized light (Figure 11A–B). In this situation, even an eventual spatially selective erasure of desired areas of the sample can be easily realized by shining an erasing beam with a spatially structured intensity profile. An example highlighting this spatial-selective optical erasure/rewrite process is given in Ref. [52], where

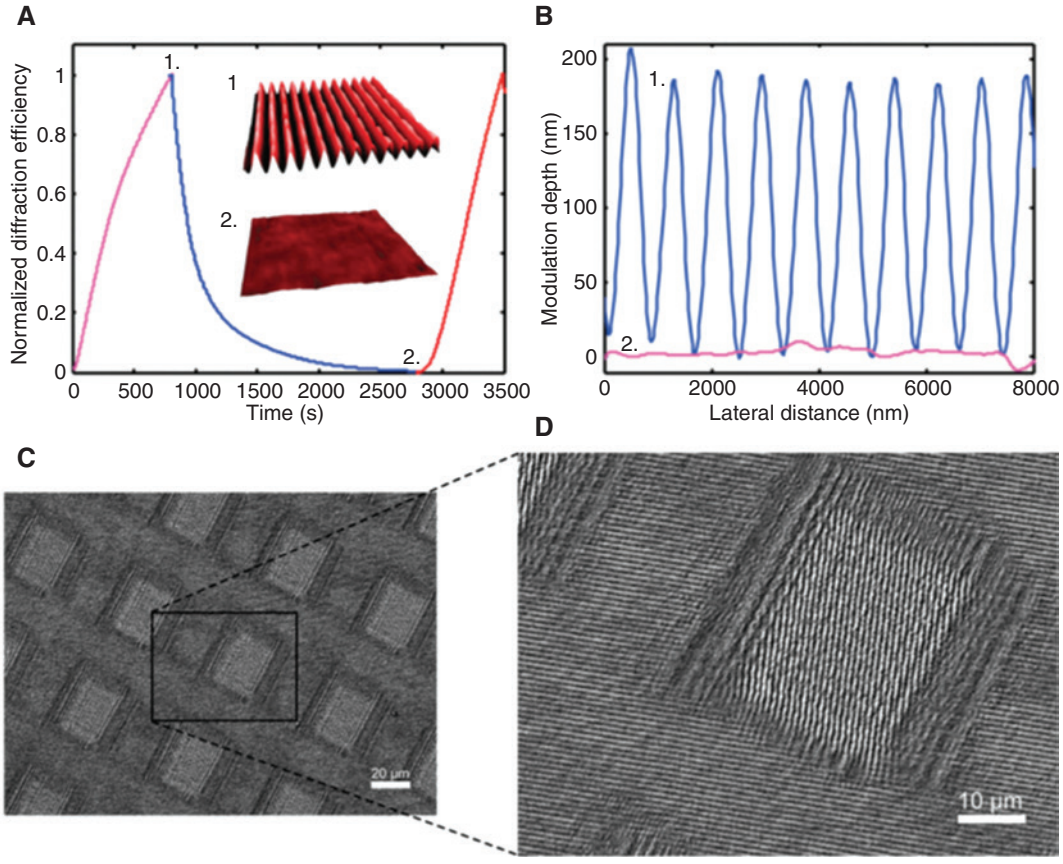

Figure 11: Erasure and rewriting of SRGs in different directions.
(A) Normalized first-order diffraction efficiency relative to one-dimensional SRG inscription (magenta), optical erasure (blue) and rewriting (red) processes in a supramolecular azomaterial. The inset shows 3D AFM images of the inscribed (1) and the erased film (2), while their topographic profiles are presented in panel (B) by the blue and magenta curves, respectively. (C–D) Scanning electron microscopy images of the spatially structured azomaterial surface created by first optically erasing a previously inscribed SRG through a transmission mask and then rewriting a new SRG pattern through the same mask. Reproduced from Ref. [76] with permission from the Royal Society of Chemistry.

previously inscribed SRGs are deleted and then rewritten with a new grating vector only in specified areas of the film through the use of a transmission mask (Figure 11C–D).

3.2.3 Applications of the SRGs

Many of the technological applications of the periodic modulations induced by the light onto the surfaces of the azomaterial films exploit the physical proprieties gained by the textured surfaces in respect to the flat azomaterial films. In such applications, the structured azomaterial films can be used directly as obtained after the light structuring exposure or can be used as molding templates and lithographic masks for the transfer of the superficial texture on other materials.

The surfaces with 1D sinusoidal SRGs are characterized by significant structural anisotropy, with a preferential direction represented by the direction of the grooves. A similar structural anisotropy translates also in anisotropy in the superficial properties like wettability and adhesion, both strongly dependent on the actual spatial configuration of the superficial roughness. A report about the use of a patterned 1D SRGs as a substrate with controlled anisotropic wettability is found in Ref. [199]. The direction parallel to the grooves in a 1D textured surface, like the 1D SRG, represents a preferential direction along which liquid volume can anisotropically propagate [200, 201]. The deposition of a liquid drop on such anisotropic surface results hence in asymmetric elongation of the liquid contact line (Figure 12A) (triple-phase contact line, TLC), which is quantified by an anisotropy in the observed liquid contact angle along different directions of the substrate (Figure 12B–C). The degree of wetting anisotropy of the texture depends explicitly on the modulation depth and on the periodicity of the rough surface [199, 203]. Both these structural parameters are easily tunable through the control of the irradiation parameters in the light-induced SRG inscription process, making the SRGs an easy and cost-effective fabrication framework of

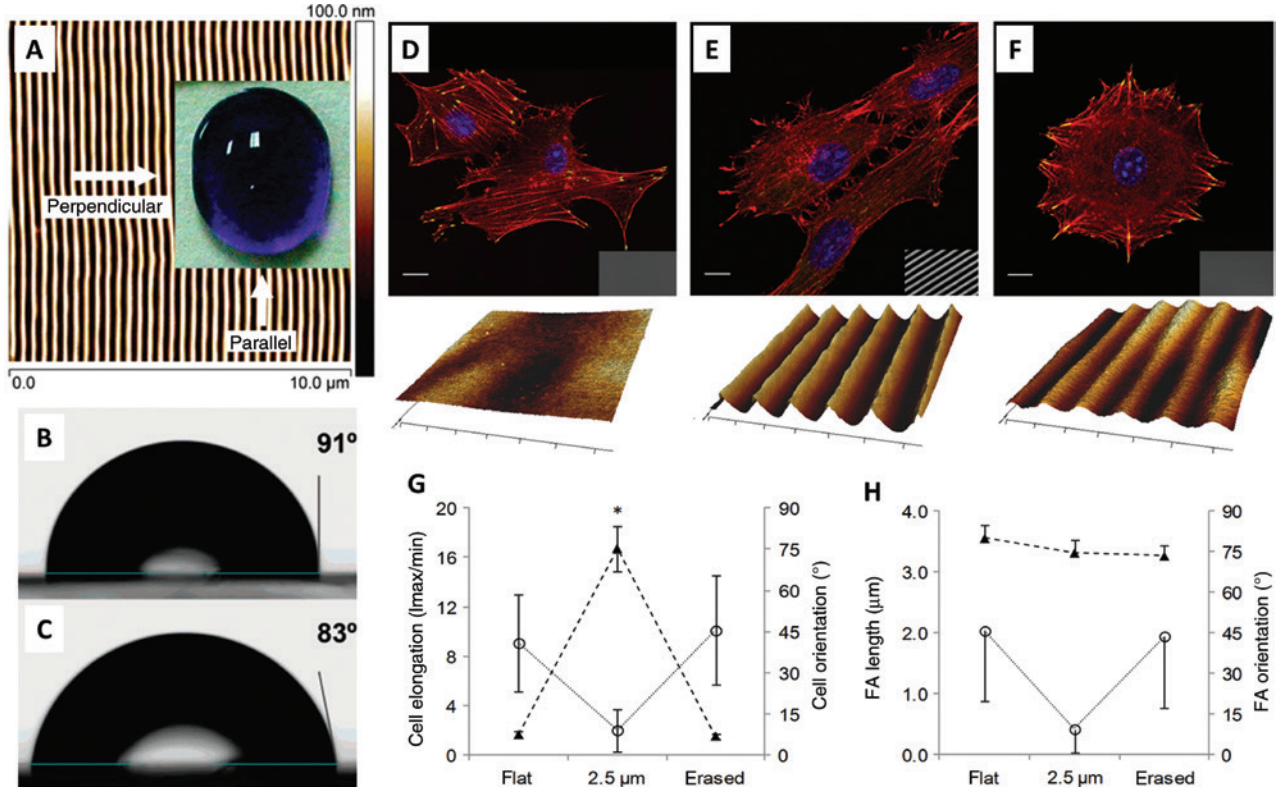

Figure 12: Anisotropic wettability and adhesion properties of sinusoidal 1D SRGs.
(A) Topographical AFM image of a sinusoidal SRG and (inset) top view of a 5-µl water droplet containing blue dye. (B) and (C) Side views of the droplet seen from the direction parallel and perpendicular to the SRG grooves, respectively. Adapted with permission from Ref. [199], copyright 2007, American Chemical Society. Confocal images of NIH-3T3 cells cultivated on (D) flat azopolymer substrate, (E) patterned sinusoidal SRGs, (F) erased SRGs. Scale bars: 10 µm. (G) Plots of cell elongation and cell orientation. (H) Plots of the FA length (▲) and orientation (○). Reproduced with permission form Ref. [202], copyright 2015, American Chemical Society.

large-scale periodic patterned substrates for fundamental studies about anisotropic surface wettability [199] and their applications [204].

Another situation where the modulated anisotropic texture of the 1D SRG presents advantages with respect to other micro- and nanofabrication techniques concerns the study of the substrate-influenced behavior of living cells [202, 205–211]. A large number of works emphasize, indeed, the role of the substrate topographic pattern in influencing cell properties like attachment, spreading and differentiation [212, 213], opening the way to crucial advances in clinical and tissue bioengineering. Besides the ability of producing controlled large-scale micro-textures whose geometry directly affects cell behavior, the optically induced surface reliefs in the azomaterials add also to the unique possibility of dynamic light-induced reconfiguration of the inscribed superficial textures. This aspect makes the surface reliefs particularly attractive for the investigation of the dynamical response of the cell properties to time-varying controlled topographical stimuli. An example of cells elongated and reoriented from the interaction with a biocompatible SRG support is presented in Figure 12D–E, while Figure 12F shows the image of a cell grown on the optically erased SRG, which recovers the initial structural properties of the cells directly grown on the flat pristine azopolymer substrate (Figure 12G–H).

The research field where SRGs find many other applications is photonics [77, 80]. The applications related to the direct use of azopolymer SRGs as photonic elements are typically based on their tunable and efficient properties as diffraction gratings [68, 72, 83, 214–217]. SRGs acting as Bragg reflectors have been largely used as light couplers and spectral filters [218–224]. In these optical devices, the modulated surface of the azopolymer enhances the coupling of the propagating light in waveguided modes at specific wavelengths, resulting in resonant peaks in the angular reflection and transmission spectra, which depend also on the periodicity of surface texture. The waveguided coupling can be obtained in the textured azopolymer film itself (Figure 13A) or in a slab of another material onto which the textured azopolymer film is deposited (Figure 13B). Other fabrication designs can involve also the deposition of materials with enhanced optical properties onto the light-induced SRGs [226, 227].

The diffractive properties of the periodic superficial texture of the SRGs can be used also to realize the optical feedback mechanism necessary for the operation of the distributed feedback lasers (DFB lasers). In such mirrorless lasers, the optical feedback is provided by Bragg scattering, which originated from periodic perturbations in the gain and/or refractive index of the active medium, while the emission wavelength depends on the period of such modulations [228, 229]. Organic DFB lasers based on the SRG induced onto azomaterial surfaces can be easily realized by covering the inscribed SRG with a layer of active material, giving rise to a stacked structure presenting a spatially modulated effective refraction index [230–232]. Other fabrication possibilities concern the effective modulation of gain of an active layer obtained from the direct inscription of the SRG onto a fluorescent-doped azomaterial film. An example of such a device is found in Ref. [225], while its operating principle, able to transform the amplified spontaneous emission (ASE) in laser emission, is shown in Figure 13C–F. Despite the fact that fluorescence quenching can be a limit for the performance of DFB lasers realized through this SRG-based design, it has the remarkable advantage of direct tunability of the emission wavelength by the proper choice of the fluorophores and grating periods (Figure 13D). Furthermore, it should be mentioned that some of the problems associated to fluorescence quenching and fluorophore bleaching occurring during the SRG structuring have been overcome in recent works that reported about the use of azomaterials for the holographic inscription of refractive gratings (polarization gratings) instead of SRGs [233–238]. Even if the process does not involve mass migration phenomenon but only the photo-reorientation of the azochromophores, the successful application of such polarization grating for DFB lasing widens considerably the range of possible azobenzene-based materials suitable for this application.

Many other applications in photonics, as well as in other technological fields, could in principle take advantage from the periodic textured surfaces of both 1D and two-dimensional (2D) SRGs inscribed in azomaterial films. For example, controlled textured surfaces acting as light-harvesting layers can be used to improve the performances of solar cells [239, 240] and other optoelectronic devices [241–243], to record holograms [244, 245] or to mimic the structure of some functional surface found in nature [246]. Recently, SRGs have been even used as patterned electrodes for the fabrication of flexible light-healable triboeletric generators [247], which can find applications in the emerging technological field of wearable electronic devices.

In several practical situations, especially related to the design of optical devices with enhanced performances, the direct use of a layer of photosensitive azomaterial can deteriorate structural stability as a consequence of undesired mass migration effects. Moreover, the azomaterial layers are not optically transparent in the UV/visible portion of the light spectrum [216], and their direct use in

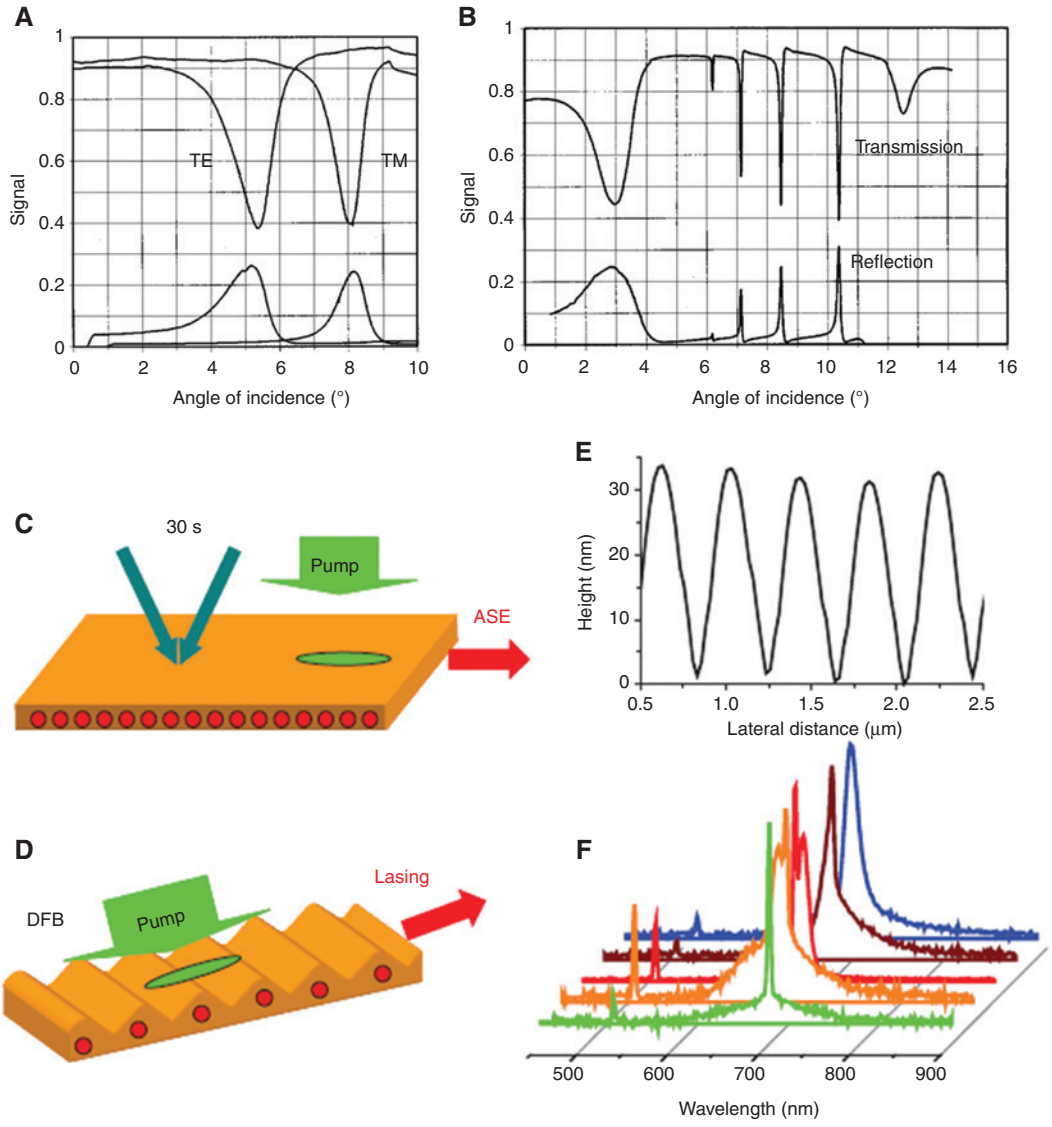

Figure 13: Applications of the SRGs as diffractive optical elements.
(A) Normalized angular transmission (top) and reflection (bottom) spectra of a TM and a TE polarized He-Ne beam propagating through a 500-nm-thick azopolymer layer presenting an SRG with pitch of 390 nm. (B) When the azopolymer layer is deposited onto a polyamide waveguide, the angular spectra for the TE polarized beam present sharp features, demonstrating a resonant coupling of the light in waveguided modes. Reprinted from Ref. [219] with permission from AIP Publishing. (C–D) A distributed feedback (DFB) laser fabricated by a dye-doped structured azomaterial film. The SRGs inscribed onto the film provide the optical feedback that switches the amplified spontaneous emission (ASE) in a laser emission. (E) AFM height profile of SRGs inscribed on the emitting material blend. (F) Laser emission spectra obtained by tuning the SRG periodicity for different dyes included into the azomaterial. Reproduced from Ref. [225] with permission from John Wiley and Sons, copyright 2012.

optical devices can limit the wavelength operation range outside the azobenzene absorption bands. However, such limitations can be easily overcome by transferring the light-induced texture of the structured azomaterial surface onto other organic or inorganic materials, having eventually different chemical, optical, electronic and thermal properties in respect to the original azomaterial films. The pattern transferring onto organic materials generally involves a soft lithographic approach [248–251] in which the light-induced SRGs inscribed onto the azomaterial film are used as master templates for the fabrication of elastomeric stamps by a replica molding process [252]. Typically, stamps are made of poly(dimetylsiloxane) (PDMS), a material platform that allows the reproduction of the complementary superficial SRG texture with high fidelity (Figure 14).

The fabricated stamps then can be either used themselves as functional substrates or can serve as molding

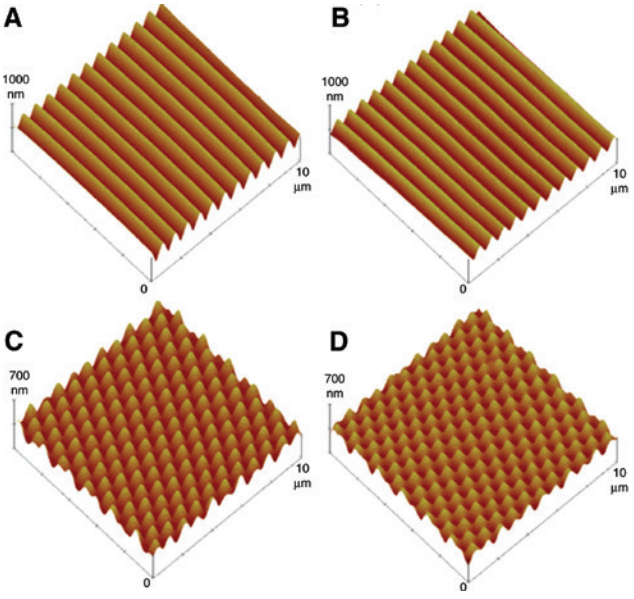

Figure 14: Soft lithographic replica of azopolymer SRGs through PDMS stamps.
AFM images of the azopolymer masters (A and C) and relative PDMS replica (B and D) for one-dimensional and bi-dimensional SRGs. Adapted with permission from Ref. [252], copyright 2006, American Chemical Society.

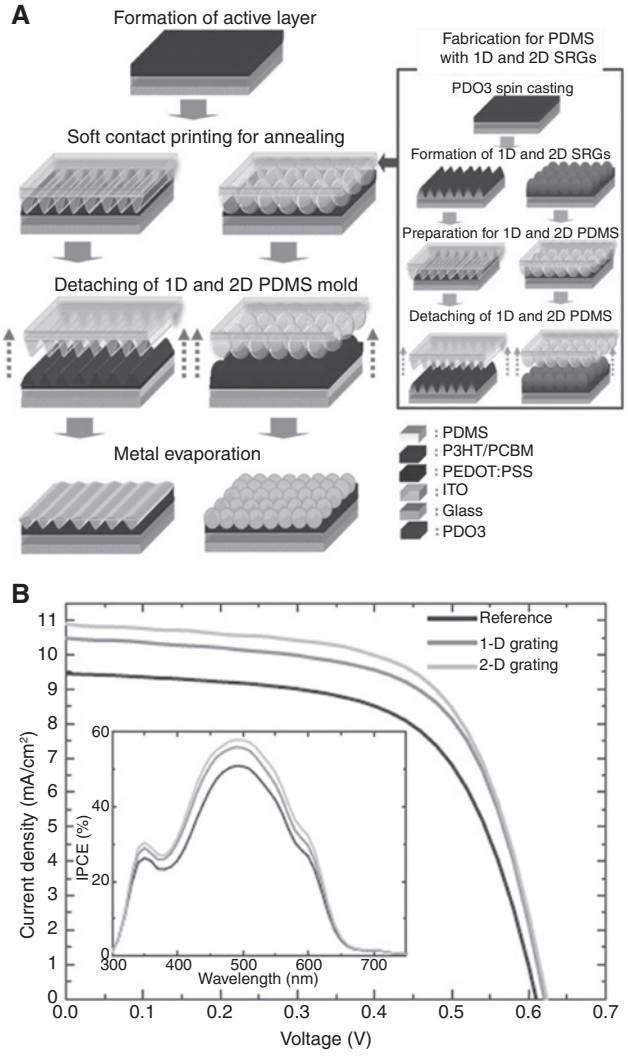

Figure 15: Use of 1D and 2D SRGs as templates for the fabrication of an organic solar cell with enhanced photon-current efficiency.
(A) Schematic representation of the solar cell fabrication sequence. The PDMS molds obtained from the SRGs inscribed onto the azopolymer are used to texture the organic active layer of the devices. (B) Comparison of the J-V characteristics for a flat active layer (reference) and the cells with 1D grating and 2D gratings (inset). The textured active layers increase the incident-photon-to-current conversion efficiency (IPCE). Adapted from Ref. [257] with permission from John Wiley and Sons, copyright 2008.

templates for the new soft-lithographic fabrication steps on other materials (e.g. photoresist or optical active layers). This approach has been successfully employed for the fabrication of transparent patterned substrates in UV-curable photopolymers, suitable for the operation of a DFB laser [253] and for the realization of microlens arrays [192]. Furthermore, the PDMS-based replica molding of 1D and 2D SRG has been also used to improve the performances of different optoelectronic devices. Taking advantage from the enhanced absorption efficiency for photons propagating in a textured active layer, organic solar cells with improved efficiency have been fabricated from SRGs templates [254–257] (Figure 15), while the replica of hexagonal SRGs onto the substrate used for the fabrication of organic light-emitting diodes (OLEDs) has been demonstrated to increase the light extraction efficiency of the LED [193, 258].

Several reports about the use of SRG as etch masks for texture transfer onto inorganic materials can also be found in the literature. In these micro-fabrication applications, the azopolymer film is typically deposited onto the flat inorganic substrate intended to be structured. The SRGs are then simply inscribed onto the azopolymer, and once the light-induced azomaterial structuration is accomplished, a chemical etching (typically realized using a reactive ion etching) of the azomaterial layer is used to partially expose some regions of the substrate, whose spatial configuration depends on the SRGs geometry. In the last fabrication step, the substrate is finally etched though the azopolymer mask by using standard wet or dry etching processes. With this approach, periodic structures ranging from groves, posts and more complex bidimensional arrays have been successfully fabricated onto metal, silicon and indium tin oxide (ITO) substrates [259–263], finding potential applications also in the fabrication of controlled scattering arrays for resolution tests of optical microscopes [264, 265].

3.2.4 Light-induced reconfiguration of pre-patterned azomaterial microtextures and microvolumes

The possible applications of the light-induced micro- and nano-structuration of azomaterial surfaces in the fields of material science and technology can be significantly enlarged by the light-induced deterministic reconfiguration of properly prestructured azomaterial films and microvolumes. There are several aspects that make the coupling of prestructuration and mass migration particularly relevant for the fabrication of complex 3D superficial micro-textures, which can extend eventually even over large areas of several square centimeters [178]. One of the most crucial points of this approach is certainly the possibility of using a very simple illumination configuration for the 3D geometrical reconfiguration of the surface. The illumination scheme, indeed, is typically constituted by just a single polarized and collimated light beam. However, despite the simple optical configuration, the range of achievable 3D geometries is very large and, in some cases, able to produce superficial textures that are difficult or even impossible to achieve with standard, and more expensive, lithographic techniques. The reconfiguration of azopolymer microstructures offers also the attractive ability to re-tune (even reversibly) several times the actual geometry of the superficial texture by means of simple all-optical steps. This aspect can represent a crucial advantage when compared to other lithographic techniques, which only rarely allow further tuning of the structures once fabricated.

The preparation of the pristine superficial microtexture onto the azomaterial film is typically accomplished by a PDMS-based replica molding process, which makes use of a lithographically fabricated master for a solvent-assisted structuration of the azomaterial surface [79, 168, 266] (Figure 16A). Such soft-lithographic azomaterial texturing has been successfully used to fabricate large-scale pristine arrays with various geometries, including parallel groves, holes, pillars (Figure 16B) and 2D microtextures in several shapes and geometrical arrangements. Similar pristine textured surfaces can be fabricated also through the all-optical patterning approach of the proximity field nanopatterning [268]. In this all-optical method, the surface structuration is achieved by irradiating a flat azomaterial film through a prestructured PDMS mask, which serves as a template for the spatially selective accumulation of the light-fueled moving azomaterial (Figure 17A). Recently, Choi and coworkers [269] showed that the quality of the optically fabricated 3D azopolymer textures can be highly improved by using two sequential light irradiation steps at slanted and normal incidence (Figure 17A–B),

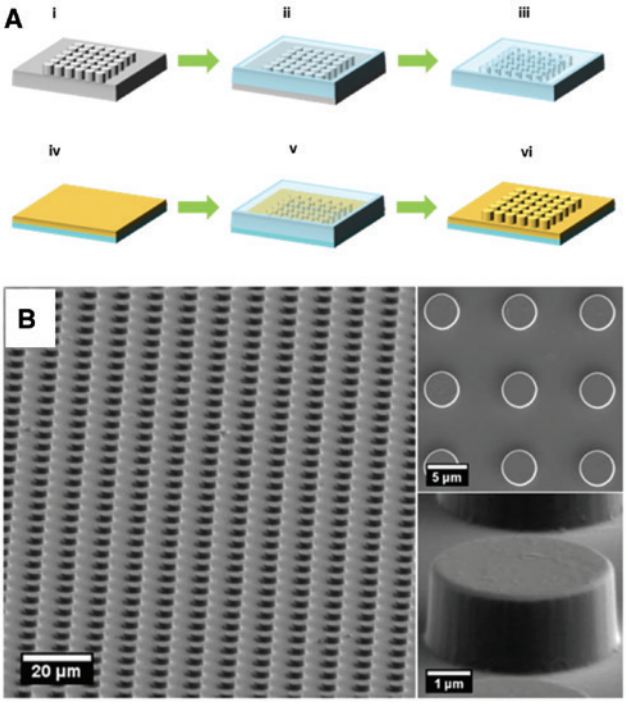

Figure 16: Preparation of solvent-assisted prestructured azomaterial surfaces.
(A) Schematic representation of the fabrication steps required for the preparation of the textured azomaterial surface. The PDMS stamp is obtained from a lithographically fabricated silicon master (subpanels i–iii) and is then used to transfer, after the solvent evaporation (iv–v), the original texture onto the polymer film (vi). (B) SEM images of an array of cylindrical micropillars fabricated by the soft-imprinting process exemplifying the high quality achievable in the replicated textures. Reproduced with permission from Ref. [267], copyright 2017, American Chemical Society.

demonstrating the proximity field nanopatterning to be a concrete alternative to the solvent-assisted preparation of high-quality prestructured azomaterial surfaces. This technique can be of particular relevance for the patterning of particular azomaterial systems, like the supramolecular azopolymers [89], in which the solvent-assisted soft-imprinting could produce the diffusion of the not strongly bonded azomolecules in the PDMS mask during the solvent evaporation, causing then a complete loss of the material photoresponse. The all-optical proximity field nanopatterning allows also a facile fabrication of complex hierarchical textures [269] (Figure 17C–F), which can be of particular interest for applications in several technological fields.

Once fabricated, the prestructured azomaterial surfaces can be reconfigured by a light irradiation step, whose phenomenology follows the general polarization-dependent directionality of the mass migration phenomenon. In particular, few trivial illumination parameters can be tuned to

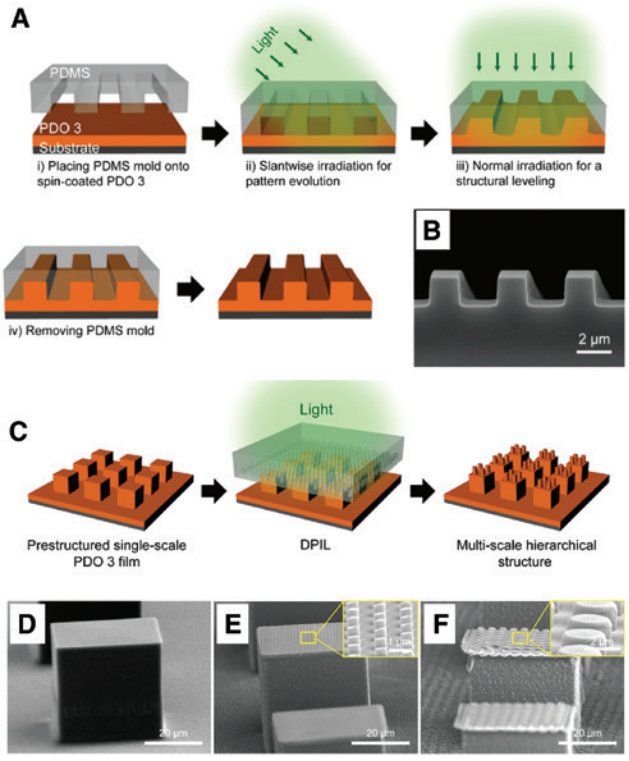

Figure 17: Fabrication of the prestructured azopolymer surfaces by means of the proximity field nanopatterning technique.
(A) Schematic representation of the illumination configuration of a flat azopolymer film through the transparent structured PDMS stamp placed in tight contact with the azopolymer surface during irradiation. This all-optical patterning method is able to produce high-quality 3D microstructures (B) and even complex hierarchical textures (C–F). Adapted with permission from Ref. [269], copyright 2017, American Chemical Society.

deterministically tailor the final reconfigured geometry of the irradiated structures. The degree of structural deformation is controlled by the light irradiation fluence [267], while the actual 3D geometry of the structures is determined by the polarization state of the irradiating light [178], with the direction of the irradiated optical electric field being the direction along which the structures become mainly deformed. Eventually, also the inclusion of some spatial constraint for the material movement at the top surface of the structures can be used to further tailor the 3D architecture of the reconfigured microstructures. This can be easily realized by capping the pristine textured surface with a transparent PDMS thin layer during the light irradiation [105, 178, 267]. Also, the incident angle of the irradiating light can be used to further tune the 3D symmetry of the reconfigured structures. As reported in Refs. [178, 267], a slanted irradiating beam induces non-uniform material motion along the polarization direction, resulting in asymmetrically reconfigured structures whose degree of directional anisotropy increases by increasing the incidence angle. Figure 18 shows the SEM images of a series of reconfigured azopolymer microstructures exemplifying the effects of different illumination conditions on the final superficial microtexture achievable starting from the same pre-patterned array of cylindrical micropillars. Figure 18A–D report the reconfigured posts obtained from the irradiation at normal incidence of the pristine array with collimated linearly and circularly polarized beams, respectively. Figure 18E–H show instead the structures obtained in the same previous irradiating polarization configurations but with the inclusion of a PDMS thin capping layer attached to the pristine structures during the reconfiguration process. This illumination configuration results in flat-top 3D reconfigured structures, having symmetric or asymmetric architecture depending on the laser polarization state. The slanted flat-top structures resulting from the irradiation of linearly polarized light at the incidence angle of 40° are shown in Figure 18I. Many other structures obtained from different pristine textures and reconfigured in similar illumination conditions can be found in the literature. These include arrays of micropillars of different sizes and shapes [168, 267, 270, 271], parallel groves [266, 272, 273] and array of microporous [274–279] and hemispherical caps [280, 281]. Another set of pristine azopolymeric structures that can be deformed with a phenomenology similar to the lithographic pre-texture surfaces pertains to the agglomerates of azopolymer colloidal particles [282–285].

3.2.5 Applications of reconfigured azopolymer microstructures

The light-reconfigurable prestructured azomaterial surfaces represent a versatile framework for the micro/nano-fabrication of complex textured surfaces, whose functionality in several applications is determined by the engineered 3D superficial roughness. For example, the 3D architecture of the light-reconfigured microstructures can be designed to sustain a strong repellence to the wetting of almost any liquid, a property commonly referred to as omniphobicity, which finds applications in several technological areas involving liquid-repellent and self-cleaning surfaces [286–288]. The realization of such strong hydrophobic surfaces requires a specific superficial texture, constituted by an array of 3D microstructures having a re-entrant geometry [289–291]. Examples coming from the natural world show that the strongest omniphobic surfaces have a double re-entrant structure, with a 3D geometry similar to a mushroom [292]. While the fabrication of such omniphobic microstructures through conventional lithographic techniques (like silicon photolithography

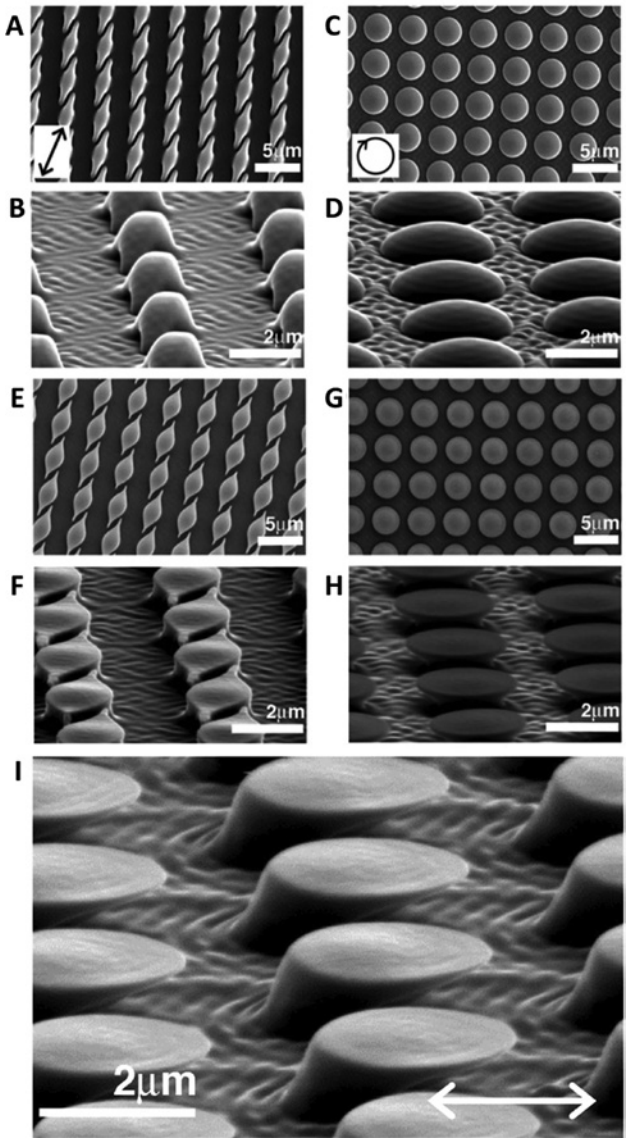

Figure 18: Azopolymer microstructures obtained from the irradiation of an array of cylindrical microposts in different configurations. (A–B) and (C–D) SEM images of the structures resulting from the irradiation of the pristine array with linearly polarized and circularly polarized beam, respectively. (E–F) and (G–H) SEM images of the flat-top structures produced in the same previous polarization configuration but including a PDMS capping layer during the light exposure. (I) SEM image of the flat-top asymmetric tilted pillars obtained under irradiation of the light at the incidence angle of $\varphi = 40°$ through the PDMS capping layer. Adapted with permission from Ref. [178], copyright 2015, American Chemical Society.

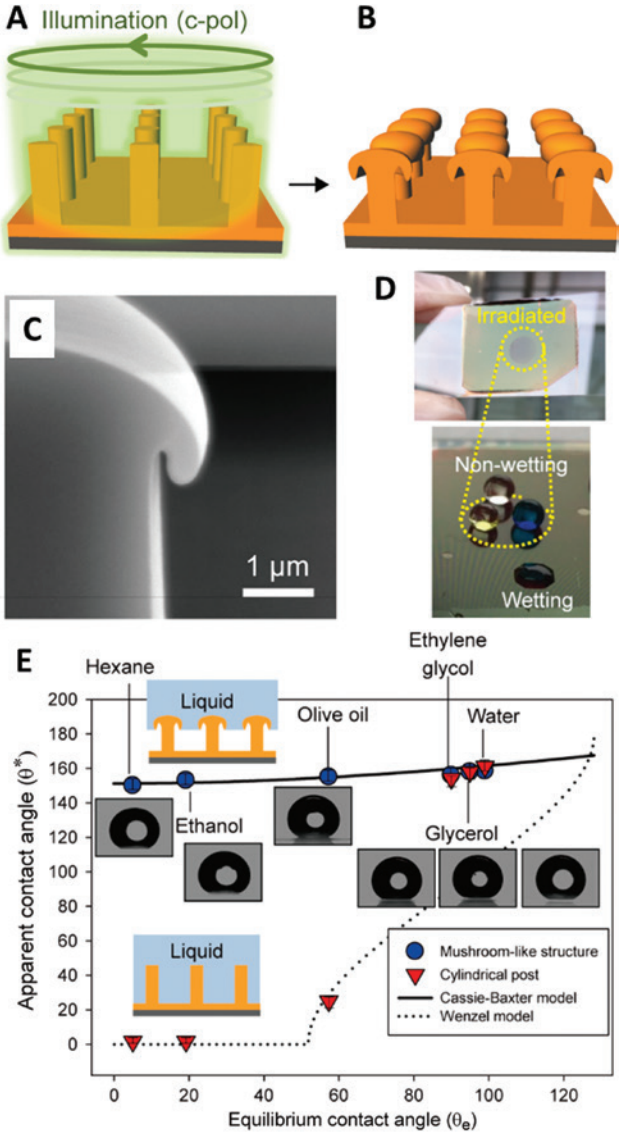

Figure 19: Mushroom-shaped azopolymer omniphobic surfaces. (A) and (B) Schematic representation of the light-induced reconfiguration of the pristine array of cylindrical imprinted micropillars. Circular polarized light is used to produce mushroom-like microstructures. (C) SEM side view of a fabricated mushroom-like pillar. (D) Photograph of the prepatterned azopolymer pillar array exhibiting an omniphobic behavior only in the irradiated regions where the mushroom-like structures are present. (E) Apparent contact angle (θ*) as a function of the equilibrium contact angle (θ_E) for the mushroom-like pillar array (denoted by the circles) and cylindrical pillar array (inverse triangles). Insets show apparent contact angles of six different liquids deposited on the mushroom-like pillar array. Adapted with permission from Ref. [294], copyright 2017, American Chemical Society.

and silicon micromachining) is highly delicate, time-consuming and expensive [290, 293], their realization can be much easier and cost-effective by using the single-step light-induced reconfiguration of array of cylindrical azopolymer microposts, irradiated with circularly polarized light [178] (Figure 19A–B). In Ref. [294], the omniphobic behavior of a reconfigured mushroom-shaped azopolymer surface has been clearly demonstrated (Figure 19C–E), showing that the light reconfiguration of azopolymeric microstructures can provide an unprecedented powerful

approach for the facile fabrication of robust, flexible and cost-effective omniphobic surfaces.

If the irradiation of an azopolymer prestructured cylindrical micropillar array with circular polarized light preserves the circular symmetry of the pristine soft-imprinted structures and affects isotopically the wetting behavior in all the directions over the surface, the asymmetric structures resulting from the irradiation of linearly polarized light [178] can induce wetting anisotropies along different directions of the film. In this case, the light polarization direction (or its projection onto the sample plane) determines, indeed, a preferential direction for the structural asymmetry and for the consequent wettability anisotropy. In Ref. [267], we reported about the accurate tailoring of the anisotropic wetting behavior of such reconfigured azopolymer surface (Figure 20A). Besides the controlled and deterministic wettability anisotropy, the same pristine array of cylindrical azopolymer micropillars has been demonstrated to achieve even tunable uni-directional anisotropic wetting by simply varying the incidence angle

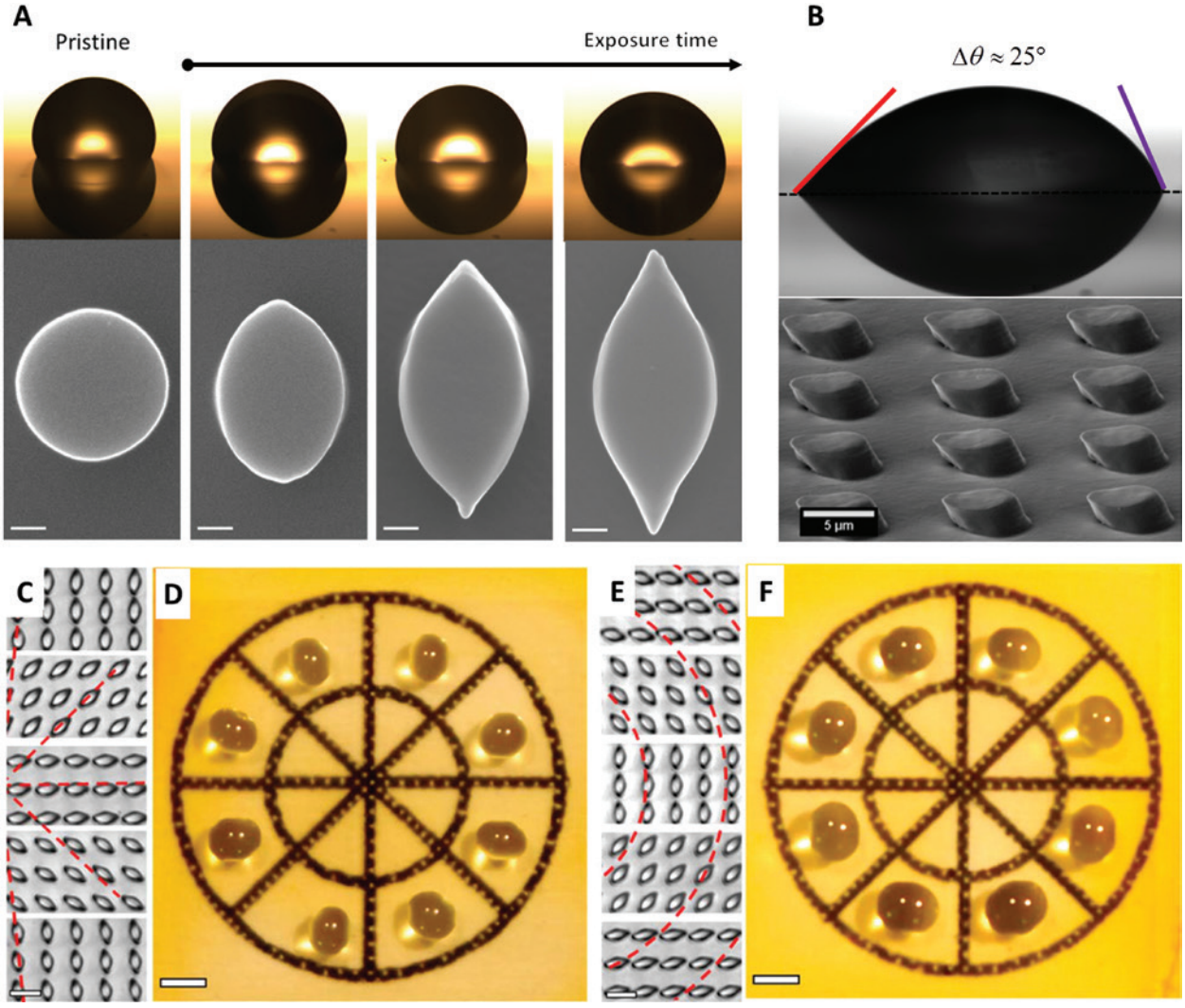

Figure 20: Anisotropic wetting behavior of azopolymer micropillars reconfigured with linear light polarization.
(A) Optical images (top) of water droplets highlighting the variation of the contact angle observed along the direction of the long axis of the asymmetric reconfigured azopolymer microstructures shown in the SEM images (scale bar: 1 μm) at increasing light irradiation time. Unidirectional left-right wetting anisotropy induced onto a liquid droplet deposited onto the array of tilted micropillar resulting from the irradiation of the pristine cylindrical micropillars at the incidence angle of $\varphi = 45°$. (C) and (E) Optical micrographs of different regions of the array of pillars reshaped with the radially and azimuthally polarized beams, respectively (scale bar: 10 μm). (D) and (F) Photographs of liquid droplets placed in different regions of the radially and azimuthally reconfigured array, respectively (scale bar: 1 mm). Adapted with permission from Ref. [267], copyright 2017, American Chemical Society.

of the linearly polarized light (Figure 20B). Furthermore, structured polarization/intensity light distributions have been successfully used to design 2D wetting pathways onto the surface of azopolymer substrate having a fixed pre-patterned geometry. Examples of arrays of radially and azimuthally oriented azopolymer micropillars, obtained over a 1-cm^2 area in a single irradiation step through radially and azimuthally polarized light beams, are shown in Figure 20C and E, respectively. The corresponding radially and azimuthally varying wetting anisotropy is highlighted by the overall elongation directions of the liquid droplets placed in different positions of the irradiated film, as shown in Figure 20D and in Figure 20F. Even if the two mentioned experiments already demonstrate the huge potential of the light-reconfigurable array of azomaterial microstructures in the wettability-oriented applications, we believe that many new applications in this field will appear in the next few years, probably further exploiting also the reversible behavior of the light-driven mass migration able to drive reversible structural deformation at command [271, 281, 295].

The light-reconfigurable pre-patterned azopolymer superficial textures can find several applications also as photonic elements able to manipulate and nano-focus the light. Mushroom-shaped dielectric microstructures, similar to the one easily achievable onto the reconfigured azomaterial cylindrical micro-posts, are known to behave as optical micro-resonators with extremely high q-factors [296, 297]. Even if studies about such azopolymer micro-resonators have not been reported yet, we believe that there are no particular conceptual limitations for this application. Imprinted pre-patterned azomaterial surfaces can also be used in the fabrication of hierarchical structures, in which the 1D or 2D nanometric texture of the SRGs is inscribed directly onto the surface of azopolymer micro-post arrays or onto large-scale azopolymer wavy surfaces. Such light-reconfigurable hierarchical textures have been demonstrated to be able to precisely control light reflection and diffraction properties, providing light-tunable color structuration [270, 298] and enhanced OLED outcoupling efficiency [298]. In Ref. [299], the reconfigured 3D structures resulting from the irradiation of an array of sub-micron-sized holes with circularly polarized light are used as templates for the fabrication of 3D tapered Au nanoholes (Figure 21A). Such metallic nanostructures have been proven, both theoretically and experimentally, to provide light nano-focusing (Figure 21B–E), opening to the use of such light-reconfigured structures in surface-enhanced Raman spectroscopy (SERS) [300] and in integrated nano-optical circuitry [301].

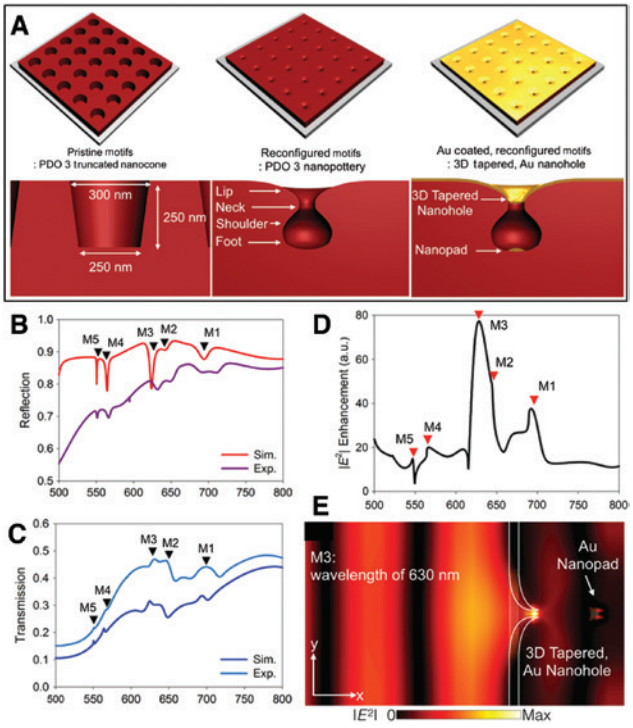

Figure 21: Light nano-focusing through the reconfigured array of nano-holes covered by a thin metallic layer.
(A) Schematic representation of structure of the 3D tapered metallic nano-hole array obtained from the reconfiguration of a prestructured array of cylindrical azopolymer holes. Both experimental and simulated reflection and transmission spectra of the metallic nano-hole array presented in (C) and (D) show the presence of resonant plasmonic modes. The plasmonic mode M3 is expected to have high enhancement in the nano-hole (D), providing strong nano-focusing (E). Adapted from Ref. [299] with permission from Wiley and Sons, copyright 2014.

4 Light-induced deformation in films of azobenzene-containing LC elastomers

Another class of materials in which the nanoscopic light-induced isomerization of the azobenzene molecules is transferred into a macroscopic movement involves azo-LCEs. LCEs are loosely cross-linked polymer networks that share the properties of both liquid crystalline polymers and elastomers [302]. Similar to normal LCs, LCEs are characterized by an ordered organization, in which the molecular constituents of the material are preferentially aligned in a liquid crystalline phase. In addition, the design of an LCE architecture involves the inclusion of slightly dense crosslinks, which confer specific structural and elastic properties to the polymeric network. Such materials are then solid polymeric systems, cuttable in

free-standing films with well-defined shapes, possessing furthermore a defined molecular order. The peculiarity of LCE films is the large structural deformation they undergo in response to an external stimulus capable to disrupt the molecular liquid crystalline order. The competitive mechanism is obviously the heat transfer to material matrix. A temperature increase, indeed, can cause liquid crystalline into isotropic phase transition, turning the ordered material system into a disordered one. The increase of structural disorder at molecular level translates into a macroscopic contraction of the LCE along the LC director, which defines the direction of the molecular alignment, and the concomitant material expansion in the direction orthogonal to the director. As this structural deformation is reversible, LCEs have immediately been regarded as soft actuators and artificial muscles able to convert at command external energy into mechanical movement. A particularly relevant aspect associated with the technological implications of LCEs is that the reversible structural deformation can be driven even using light as energy source once the azobenzene molecules have been included into the material matrix. In this case, indeed, the non-mesogenic *cis*-azobenzene isomer produced into the photoisomerization destabilizes the initial LC phase, efficiently sustained by the rod-like *trans*-azobenzene, and causes the lowering of the LCE molecular order, which eventually leads to the macroscopic material deformation. Furthermore, as the photoisomerization reaction is fully reversible, the initial geometrical configuration of the LCE film is restored by the thermal relaxation of the *cis*-azomolecules back to the mesogenic *trans* isomers. The relaxation induces a recovery of the original LC phase and makes the material available for a new photo-actuated deformation. Eventually, the LC order recovery can be also accelerated by the irradiation of the LCE film with visible light, which further stimulates the depletion of the *cis*-azomolecule population. Reversible light-induced uniaxial contraction of about 20% along the director direction of monodomain azobenzene-containing LCEs has been reported since the first studies about the light-induced mechanical actuation of these materials [303, 304]. However, the exact geometry of the film deformation depends on the actual distribution of the LC directors inside the film, and in azobenzene-containing LCEs, it can be different for monodomain and polydomain liquid crystalline networks. Details about LCE chemistry, design, molecular alignment strategies and macroscopic deformation engineering can be found in several already existing reviews [32, 305–311]. Here, we want to provide a general and brief overview on the main aspects of the photo-actuation occurring in azo-LCEs as a manifestation of a nanoscopic-to-macroscopic propagation of light-induced movements in azomaterials, highlighting also several applications offered by such material systems as light-driven artificial muscles, self-propelling locomotors and energy-harvesting devices.

4.1 The photo-actuation in azo-LCEs

The light-induced deformation of a free-standing monodomain azo-LCE films (typical thickness in the order of 10–100 μm) involves typically the bending of the film toward the direction of the incoming irradiating light [312–315]. Such bending behavior is determined by the large absorption extinction coefficient of the *trans*-azomolecule in the UV optical range, which generates a gradient in the photoisomerization efficiency for the azomolecules located at different positions along the direction of the film thickness. Indeed, most of the incident light is absorbed in the proximity of the irradiated surface within a thickness of 1–2 μm, while the *trans*-azomolecules in the bulk of the film and at the bottom surface remain almost unaffected [312]. This isomerization gradient causes the contraction only of the exposed surface of the film, which finally bends toward the incoming light direction (Figure 22).

A large range of strong and complex photo-actuation modes can be achieved by controlling such bending behavior by means of an accurate spatial patterning of the molecular orientation directions across the film. For example, using a splay alignment of the mesogens (Figure 23A), the degree of structural bending is increased in respect to the monodomain ordered matrices [316, 317], while the bending direction of the film with this molecular alignment depends on which surface of the film is exposed to the light (Figure 23B–F) [318]. Even very complex 3D programmable deformations of the LCE films can be obtained by accurately patterning the molecular alignment into two dimensions. Examples from literature show geometrical deformations similar to waves, springs, cones and saddles [66, 67, 319–321], opening the way to the arbitrary tailoring of the actuation geometry by means of a careful control over the molecular alignment [32, 311, 322, 323].

Differently from LCE monodomains, the bending direction of azobenzene-containing polydomain LCE films is determined by the direction of the irradiating linearly polarized light [324]. In a polydomain LCE, the alignment direction is uniform only at the microscale, while macroscopically, the direction of the molecular alignment is essentially random. Each micro-domain of an azo-LCE contains *trans*-azomolecules oriented along the local

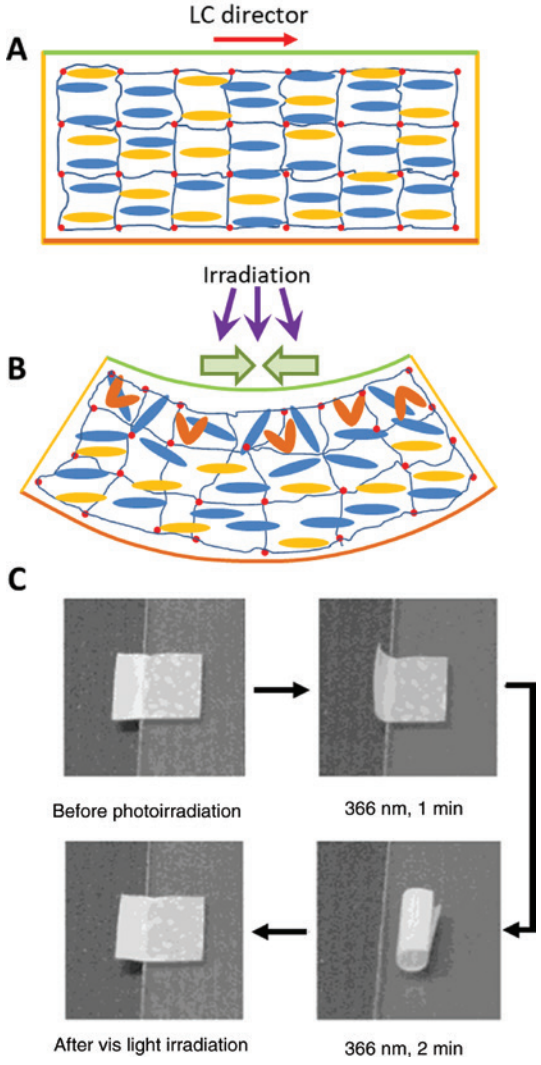

Figure 22: Photoinduced bending of an azo-LCE film along the LC director.
(A) Schematic illustration of the molecular arrangement of cross-linked LC network (crosslinks represented by red spots) constituted by non-photoresponsive mesogens (blue) and azomolecules (yellow). (B) Schematic illustration of the photo-isomerized gradient of azomolecules along the direction of the film thickness causing the bending of the LCE film. (C) Bending and unbending behavior of an azo-LCE film along the molecular alignment direction irradiated with UV and visible light (adapted with permission from Ref. [313], copyright 2004, American Chemical Society).

molecular director. Due to the orientation-dependent efficiency of the light absorption for the *trans*-azomolecule, the irradiation of an azo-LCE with linearly polarized light drives an efficient order-disorder transition only in microdomains where the mesogenic *trans*-azomolecules are aligned with the light polarization direction. As a result, a reversible and directional photo-selective film bending is achieved only in the direction of the linearly polarized light (Figure 24).

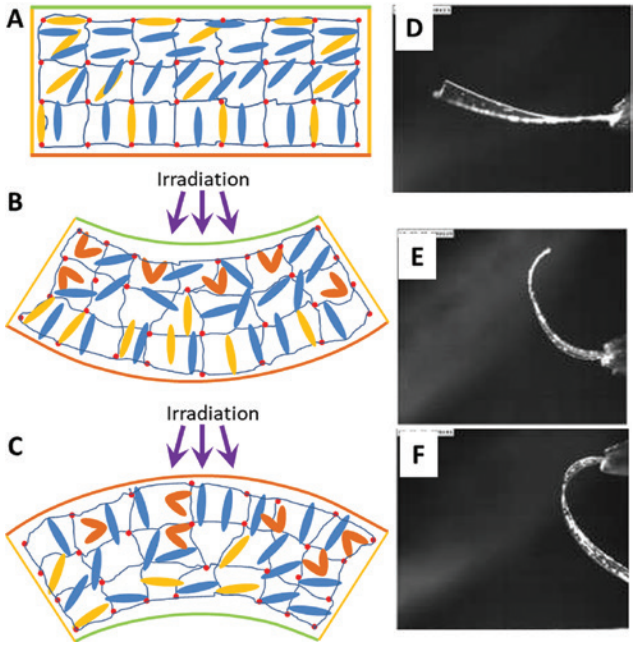

Figure 23: The bending behavior of an azo-LCE film with splayed alignment.
(A) Illustration of the molecular arrangement. If the film is irradiated exposing the surface (green) with planar alignment, the film bends upward (B). On the contrary, if the surface exposed has homeotropic alignment (orange), the film bends downward (C). (D–F) Experimental bending behavior of an azo-LCE film with splay alignment showing increased bending in respect to a fully planar film (D) and the inversion of the bending direction if illuminated at planar (E) and homeotropic (F) sides. (D–F) Adapted with permission from [316], copyright 2007, Springer Nature.

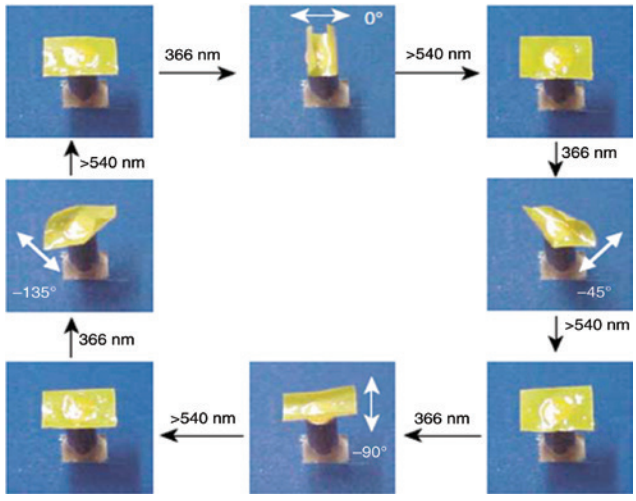

Figure 24: The polarization-dependent bending and unbending behavior of polydomain azo-LCE films.
The bending direction is determined by the direction of the irradiated linearly polarized UV light. Adapted with permission from Ref. [324], copyright 2003, Spinger Nature.

4.2 Light-fueled robots and actuators

Light-fueled azo-LCE actuators can present several advantages with respect to electrically driven ones because they convert light energy directly into mechanical work without the aid of batteries, electric contacts or electrical engines. In several reported applications, the use of azo-LCEs as light-driven actuators requires a controlled irradiation of light at two wavelengths, able to fuel at command the disruption of the molecular alignment and the acceleration of its recovery via the photoisomerization reactions of the azomolecules. For more complex deformation modes and functionalities, also localized and spatio-temporally modulated irradiating light can be used.

Simple examples of light-to-mechanical energy conversion accelerated by the wavelength switch of the irradiating light have been already given in the previous section describing the light-induced bending and unbending behavior of different LCE films [312, 313, 315, 324–326]. However, using the same approach, the photocontrolled deformation of azo-LCEs can be transferrable into the generation of actual mechanical work in clever experimental configurations. A light-fueled motor has been realized through a ring of an azo-LCE obtained connecting together the ends of a flat single-layer stripe of the elastomer [327]. The simultaneous irradiation of UV and visible light at different positions across the ring has been demonstrated to cause the local expansion and contraction of the material, which drives the rotation of the ring and even the actuation of pulleys, realizing in fact a motor fueled only by light [327].

The design of the macroscopic deformation by the molecular alignment patterning and the selective actuation with spatio-temporal modulated light can be used to drive complex structuration and motion of LCE films, which can act, for example, as light-driven switchable adhesives [328, 329], microvalve and micropumps for microfluidic applications [330, 331], robotic arms [332–334] and biomimetic locomotors. A light-driven micro-robot (Figure 25A), able to pick, lift, move and place an object heavier than its weight, has been reported in Ref. [333]. The robot constitutes three stripes of a bilayer LCE film, joined together to form a photo-actuable arm endowed with a wrist and a hand (Figure 25B). Each section of the robot can be selectively activated by switching on and off a spatially localized illuminating spot of visible light. This is a clear example in which a light-fueled soft robot can be artificially manipulated to perform some action on its environment, acting similarly to an artificial muscle. Recently, even the possibility of automatic smart-responsive robots

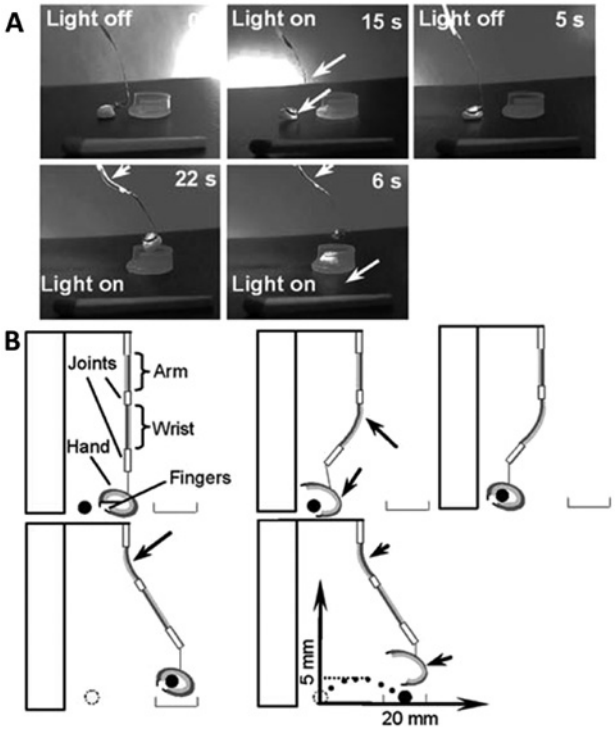

Figure 25: Robotic photo-actuated LCE arm.
(A) Photographs of the robotic arm manipulating an object weighing 10 mg. (B) Schematic illustrations of the actions of the robot shown in (A). Reproduced from Ref. [333] with permission from the Royal Society of Chemistry.

has been highlighted by Zeng and coworkers. They demonstrated the realization of a self-regulating LCE iris, whose structure deforms similarly to the iris of the human eye, which regulates the amount of transmitted light on the basis of the incident light intensity level [67]. The same group proposed also a smart azo-LCE robot able to selectively distinguish, and eventually grab, different objects on the basis of their absorption properties, as a natural flytrap does with insects and other random particles [335].

Another application scenario for azo-LCEs is the biomimetic light-induced locomotion of soft robots. This technological field has been recently reviewed elsewhere [310, 336]. In Figure 26, two examples of azo-LCE films actuated by a scanning laser beam able to drive a directional macroscopic displacement are reported. The robots mimic the natural locomotion modes of millimeter-sized walking caterpillars (Figure 26A–D) and swimming flat fishes (Figure 26E–F). The motion of such robots is provided by the activation of structural deformations of the LCE film by means of spatially or temporally modulated light patterns, able to induce the non-reciprocal deformations necessary for the directional locomotion at different positions of the robot body. Several other examples of similar

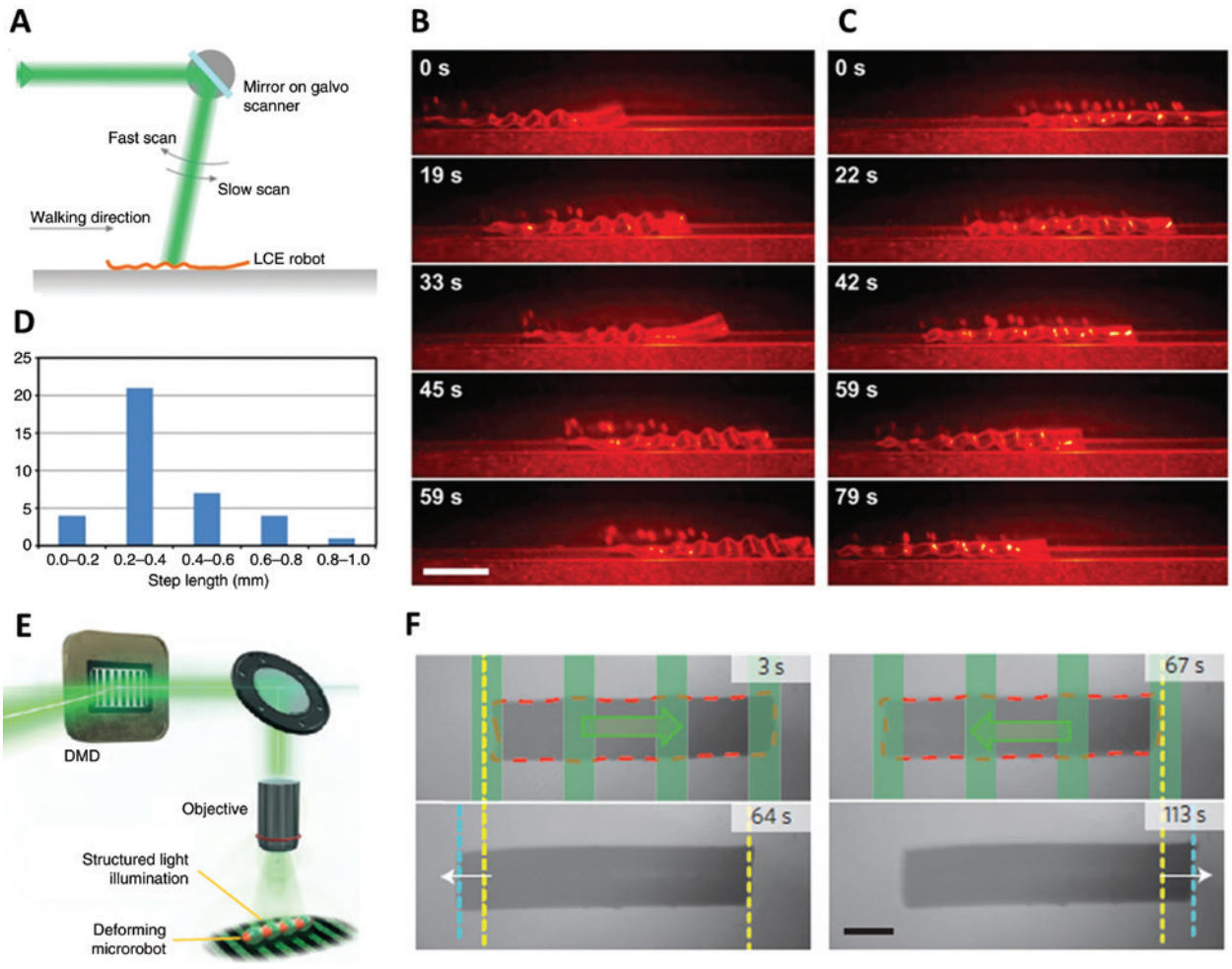

Figure 26: Light-fueled walking and swimming azo-LCE robots.
(A) Schematic representation of the experimental setup. A laser spot is repeatedly scanned across the LCE film producing forward (B) and backward (C) walking steps (Scale bar: 5 mm). (D) Histogram of the step length. (A–D) Reproduced from Ref. [319] with permission from John Wiley and Sons, copyright 2016. (E) Spatially and temporally modulated light pattern scanned across a microrobot though a digital micromirror device (DMD). (F) The robot swims in the direction opposite to that of the travelling light wave (Scale bar: 200 μm). (E–F) Adapted with permission from Ref. [337], copyright 2016, Springer Nature.

walking and swimming biomimetic azo-LCE robots can be found in the literature [314, 332, 337–340], accessing even to the micrometer spatial scale [341]. However, even stationary illumination light fields have been demonstrated to generate continuous movement and locomotion of an LCE film incorporating azomolecules with fast *cis*-to-*trans* thermal relaxation dynamics. An example of continuous wave-like deformations obtained under stationary illumination conditions in an LCE film with splayed alignment has been recently reported by Gelebart et al. [342, 343]. The light-induced continuous motion has been explained in terms of a self-shadowing mechanism initiated by the fast photo-driven deformations of the films at different positions under constant irradiation. Such effect is very promising for the realization of remotely controlled light-driven devices exhibiting interesting functionalities, like self-cleaning and self-propelling directional locomotion [342, 344]. The self-shadowing feedback mechanism from which a continuous movement originates under stationary illumination conditions is potentially of great interest also in energy-harvesting applications, where the mechanical energy of the continuously oscillating LCE films [345–347] can be converted in other forms of energy, e.g. electricity [348]. In this regard, the possibility of directly using the light coming from the sun to activate photo-driven motions like bending [349] and high-frequency and chaotic oscillations [346, 350] in azobenzene-containing LCE films can represent a new frontier for the applications of these materials for the realization of solar energy-harvesting devices.

5 Summary and outlook

Due to the efficient and reversible light-induced isomerization involving the significant variation of molecular electrochemical and structural properties, azobenzene molecules can act as versatile molecular photo-switches for materials in which they are included. Several azomaterial systems able to harness the microscopic motion of the isomerizing azomolecules in light-controllable optical, chemical and mechanical properties have been synthesized over the years. In the present review, we have described two classes of properly designed azomaterial systems in which the light-induced azobenzene molecular dynamics at the nanoscale is propagated at macroscopic spatial scales. In particular, we have mainly focused attention on the light-induced mass migration phenomenon occurring at the surface of films of amorphous azobenzene-containing materials. In such materials, the irradiation of Uv/visible light directly translates into the appearance of topographic surface reliefs, whose structural features depend on the intensity and polarization distributions of the irradiating light and on the pristine geometry of the irradiated azomaterials surface. These classes of azomaterials represent a versatile platform for light-induced micro- and nanopatterning of surfaces. Here, we have reviewed several scenarios in which the light-textured azomaterial surfaces have been used. Applications range from the photochemical imaging of optical fields at nanometric spatial resolution, to the light-induced reconfiguration of flat and pre-patterned surfaces for wettability, adhesion, photonics and lithography. New applications in all these fields will surely come in the future by exploiting new material design strategies for efficient and large surface modulation, complex illumination/prestructuration configurations and even the reversible nature of the phenomena involved. However, a further widening of their applicability would also come from the unveiling of the exact mechanism, bridging the initiator light-fueled motion of the isomerizing azomolecules and the macroscopic material transport, which is still an open question related to fundamental light-matter interaction at the basis of such nanoscopic-to-macroscopic motion propagation.

In addition, here, we described the general aspects of the photo-actuation observed in azobenzene-containing liquid-crystalline elastomers in which light is converted in controlled and reversible isomerization-initiated mechanical motion. The technological potentialities of such direct optical-to-mechanical energy conversion are enormous, and applications of azo-LCE films as artificial muscles, photo-actuators, soft robots, self-propelling locomotors, light-fueled machines and energy-harvesting devices have been highlighted. The complex photo-actuation geometries used in many of these applications are typically the result of both the accurate engineering of the patterned LC matrix and the modulation in time and/or space of the irradiating light. Future experiments will certainly explore further these design strategies to realize advanced deformation geometries and functionalities, taking advantage also from the eventual automated photo-response to external light stimuli in smart photo-driven actuators and devices. Furthermore, the continuous reversible actuation demonstrated recently in azo-LCEs with fast thermal isomerization dynamics have traced the path toward self-sustained moving light-driven actuators, which could be used in the future to continuously convert the energy of light, coming even from the sun, in mechanical or electric energy.

Acknowledgments: This study was supported by "Centro Servizi Metrologici Avanzati (CeSMA)" of the University of Naples "Federico II", Italy.

References

[1] Natansohn A, Rochon P. Photoinduced motions in azo-containing polymers. Chem Rev 2002;102:4139–76.
[2] Kumar GS, Neckers DC. Photochemistry of azobenzene-containing polymers. Chem Rev 1989;89:1915–25.
[3] Yager KG, Barrett CJ. Novel photo-switching using azobenzene functional materials. J Photochem Photobiol Chem 2006;182:250–61.
[4] García-Amorós J, Velasco D. Recent advances towards azobenzene-based light-driven real-time information-transmitting materials. Beilstein J Org Chem 2012;8:1003–17.
[5] Bandara HMD, Burdette SC. Photoisomerization in different classes of azobenzene. Chem Soc Rev 2012;41:1809–25.
[6] Bléger D, Hecht S. Visible-light-activated molecular switches. Angew Chem Int Ed 2015;54:11338–49.
[7] Lange JJD, Robertson JM, Woodward I. X-ray crystal analysis of trans-azobenzene. Proc R Soc Lond A 1939;171:398–410.
[8] Hampson GC, Robertson JM. 78. Bond lengths and resonance in the cis-azobenzene molecule. J Chem Soc Resumed 1941;0:409–13.
[9] Brown CJ. A refinement of the crystal structure of azobenzene. Acta Crystallogr 1966;21:146–52.
[10] Sato M, Kinoshita T, Takizawa A, Tsujita Y. Photoinduced conformational transition of polypeptides containing azobenzenesulfonate in the side chains. Macromolecules 1988;21:1612–6.
[11] Biswas N, Umapathy S. Density functional calculations of structures, vibrational frequencies, and normal modes of trans- and cis-azobenzene. J Phys Chem A 1997;101:5555–66.
[12] Wazzan NA, Richardson PR, Jones AC. Cis-trans isomerisation of azobenzenes studied by laser-coupled NMR spectroscopy and DFT calculations. Photochem Photobiol Sci 2010;9:968–74.

[13] Naito T, Horie K, Mita I. Photochemistry in polymer solids. 11. The effects of the size of reaction groups and the mode of photoisomerization on photochromic reactions in polycarbonate film. Macromolecules 1991;24:2907–11.
[14] Lamarre L, Sung CSP. Studies of physical aging and molecular motion by azochromophoric labels attached to the main chains of amorphous polymers. Macromolecules 1983;16:1729–36.
[15] Naito T, Horie K, Mita I. Photochemistry in polymer solids: 12. Effects of main-chain structures and formation of hydrogen bonds on photoisomerization of azobenzene in various polymer films. Polymer 1993;34:4140–5.
[16] Hartley GS. The cis-form of azobenzene. Nature 1937;140:281.
[17] Hartley GS, Fèvre RJWL. The dipole moments of cis- and trans-azobenzenes and of some related compounds. J Chem Soc Resumed 1939;0:531–5.
[18] Birnbaum PP, Linford JH, Style DWG. The absorption spectra of azobenzene and some derivatives. Trans Faraday Soc 1953;49:735–44.
[19] Kurihara S, Ikeda T, Sasaki T, Kim H-B, Tazuke S. Time-resolved observation of isothermal phase transition of liquid crystals triggered by photochemical reaction of dopant. J Chem Soc Chem Commun 1990;0:1751–2.
[20] Fujino T, Arzhantsev SY, Tahara T. Femtosecond time-resolved fluorescence study of photoisomerization of trans-azobenzene. J Phys Chem A 2001;105:8123–9.
[21] Cusati T, Granucci G, Persico M. Photodynamics and time-resolved fluorescence of azobenzene in solution: a mixed quantum-classical simulation. J Am Chem Soc 2011;133:5109–23.
[22] Rau H. In Photochemistry and Photophysics, Vol. 2. Boca Raton, FL, CRC Press, 1990, 119.
[23] Röttger D, Rau H. Photochemistry of azobenzenophanes with three-membered bridges. J Photochem Photobiol Chem 1996;101:205–14.
[24] Nagamani SA, Norikane Y, Tamaoki N. Photoinduced hinge-like molecular motion: studies on xanthene-based cyclic azobenzene dimers. J Org Chem 2005;70:9304–13.
[25] Bléger D, Schwarz J, Brouwer AM, Hecht S. O-fluoroazobenzenes as readily synthesized photoswitches offering nearly quantitative two-way isomerization with visible light. J Am Chem Soc 2012;134:20597–600.
[26] Buffeteau T, Lagugné Labarthet F, Pézolet M, Sourisseau C. Photoinduced orientation of azobenzene chromophores in amorphous polymers as studied by real-time visible and FTIR spectroscopies. Macromolecules 1998;31:7312–20.
[27] Buffeteau T, Labarthet FL, Pézolet M, Sourisseau C. Dynamics of photoinduced orientation of nonpolar azobenzene groups in polymer films. Characterization of the cis isomers by visible and FTIR spectroscopies. Macromolecules 2001;34:7514–21.
[28] Natansohn A, Rochon P, Gosselin J, Xie S. Azo polymers for reversible optical storage. 1. Poly[4'-[[2-(acryloyloxy) ethyl]ethylamino]-4-nitroazobenzene]. Macromolecules 1992;25:2268–73.
[29] Ikeda T, Tsutsumi O. Optical switching and image storage by means of azobenzene liquid-crystal films. Science 1995;268:1873–5.
[30] Tsutsumi O, Kanazawa A, Shiono T, Ikeda T, Park L-S. Photoinduced phase transition of nematic liquid crystals with donor–acceptor azobenzenes: mechanism of the thermal recovery of the nematic phase. Phys Chem Chem Phys 1999;1:4219–24.
[31] Sobolewska A, Zawada J, Bartkiewicz S, Galewski Z. Mechanism of photochemical phase transition of single-component phototropic liquid crystals studied by means of holographic grating recording. J Phys Chem C 2013;117:10051–8.
[32] Bisoyi HK, Li Q. Light-driven liquid crystalline materials: from photo-induced phase transitions and property modulations to applications. Chem Rev 2016;116:15089–166.
[33] Merino E, Ribagorda M. Control over molecular motion using the cis-trans photoisomerization of the azo group. Beilstein J Org Chem 2012;8:1071–90.
[34] Beharry AA, Woolley GA. Azobenzene photoswitches for biomolecules. Chem Soc Rev 2011;40:4422–37.
[35] Szymański W, Beierle JM, Kistemaker HAV, Velema WA, Feringa BL. Reversible photocontrol of biological systems by the incorporation of molecular photoswitches. Chem Rev 2013;113:6114–78.
[36] Trauner D, Isacoff E, Borges K, Banghart M, Kramer RH. Light-activated ion channels for remote control of neuronal firing. Nat Neurosci 2004;7:1381.
[37] Trauner D, Isacoff EY, Volgraf M, et al. Allosteric control of an ionotropic glutamate receptor with an optical switch. Nat Chem Biol 2006;2:47.
[38] Konrad DB, Frank JA, Trauner D. Synthesis of redshifted azobenzene photoswitches by late-stage functionalization. Chem Eur J 2016;22:4364–8.
[39] Bredenbeck J, Helbing J, Kumita JR, Woolley GA, Hamm P. α-Helix formation in a photoswitchable peptide tracked from picoseconds to microseconds by time-resolved IR spectroscopy. Proc Natl Acad Sci USA 2005;102:2379–84.
[40] Masiero S, Lena S, Pieraccini S, Spada GP. The direct conversion of light into continuous mechanical energy by photoreversible self-assembly: a prototype of a light-powered engine. Angew Chem Int Ed 2008;47:3184–7.
[41] Möller G, Harke M, Motschmann H, Prescher D. Controlling microdroplet formation by light. Langmuir 1998;14:4955–7.
[42] Siewierski LM, Brittain WJ, Petrash S, Foster MD. Photoresponsive monolayers containing in-chain azobenzene. Langmuir 1996;12:5838–44.
[43] Jiang W, Wang G, He Y, et al. Photo-switched wettability on an electrostatic self-assembly azobenzene monolayer. Chem Commun 2005;0:3550–2.
[44] Pei X, Fernandes A, Mathy B, et al. Correlation between the structure and wettability of photoswitchable hydrophilic azobenzene monolayers on silicon. Langmuir 2011;27:9403–12.
[45] Chen M, Besenbacher F. Light-driven wettability changes on a photoresponsive electrospun. Mat ACS Nano 2011;5:1549–55.
[46] Monobe H, Ohzono T, Akiyama H, Sumaru K, Shimizu Y. Manipulation of liquid filaments on photoresponsive microwrinkles. ACS Appl Mater Interfaces 2012;4:2212–7.
[47] Pan S, Guo R, Xu W. Photoresponsive superhydrophobic surfaces for effective wetting control. Soft Matter 2014;10:9187–92.
[48] Pipolo S, Corni S. Wettability of azobenzene self-assembled monolayers. Langmuir 2014;30:4415–21.
[49] Ichimura K, Oh S-K, Nakagawa M. Light-driven motion of liquids on a photoresponsive surface. Science 2000;288:1624–6.
[50] Feldmann D, Maduar SR, Santer M, et al. Manipulation of small particles at solid liquid interface: light driven diffusioosmosis. Sci Rep 2016;6:36443.

[51] Schimka S, Gordievskaya YD, Lomadze N, et al. Communication: light driven remote control of microgels' size in the presence of photosensitive surfactant: complete phase diagram. J Chem Phys 2017;147:031101.
[52] Schimka S, Lomadze N, Rabe M, et al. Photosensitive microgels containing azobenzene surfactants of different charges. Phys Chem Chem Phys 2017;19:108–17.
[53] Natansohn A, Rochon P, Pezolet M, et al. Azo polymers for reversible optical storage. 4. Cooperative motion of rigid groups in semicrystalline polymers. Macromolecules 1994;27:2580–5.
[54] Jiang XL, Li L, Kumar J, Tripathy SK. Photoassisted poling induced second harmonic generation with in-plane anisotropy in azobenzene containing polymer films. Appl Phys Lett 1996;69:3629–31.
[55] Nunzi J-M, Fiorini C, Etilé A-C, Kajzar F. All-optical poling in polymers: dynamical aspects and perspectives. Pure Appl Opt J Eur Opt Soc Part A 1998;7:141.
[56] Yesodha SK, Sadashiva Pillai CK, Tsutsumi N. Stable polymeric materials for nonlinear optics: a review based on azobenzene systems. Prog Polym Sci 2004;29:45–74.
[57] Virkki M, Kauranen M, Priimagi A. Different chromophore concentration dependence of photoinduced birefringence and second-order susceptibility in all-optical poling. Appl Phys Lett 2011;99:183309.
[58] Virkki M, Tuominen O, Forni A, et al. Halogen bonding enhances nonlinear optical response in poled supramolecular polymers. J Mater Chem C 2015;3:3003–6.
[59] Eich M, Wendorff JH, Reck B, Ringsdorf H. Reversible digital and holographic optical storage in polymeric liquid crystals. Makromol Chem Rapid Commun 1987;8:59–63.
[60] Berg RH, Hvilsted S, Ramanujam PS. Peptide oligomers for holographic data storage. Nature 1996;383:505–8.
[61] Hrozhyk UA, Serak SV, Tabiryan NV, Bunning TJ. Photoinduced isotropic state of cholesteric liquid crystals: novel dynamic photonic materials. Adv Mater 2007;19:3244–7.
[62] Corvazier L, Zhao Y. Induction of liquid crystal orientation through azobenzene-containing polymer networks. Macromolecules 1999;32:3195–200.
[63] Sun S-T, Gibbons WM, Shannon PJ. Alignment of guest–host liquid crystals with polarized laser light. Liq Cryst 1992;12:869–74.
[64] Leclair S, Mathew L, Giguère M, Motallebi S, Zhao Y. Photoinduced alignment of ferroelectric liquid crystals using azobenzene polymer networks of chiral polyacrylates and polymethacrylates. Macromolecules 2003;36:9024–32.
[65] Shannon PJ, Gibbons WM, Sun ST. Patterned optical properties in photopolymerized surface-aligned liquid-crystal films. Nature 1994;368:532–3.
[66] Ware TH, McConney ME, Wie JJ, Tondiglia VP, White TJ. Voxelated liquid crystal elastomers. Science 2015;347:982–4.
[67] Zeng H, Wani OM, Wasylczyk P, Kaczmarek R, Priimagi A. Self-regulating iris based on light-actuated liquid crystal elastomer. Adv Mater 2017;29:1701814.
[68] Rochon P, Batalla E, Natansohn A. Optically induced surface gratings on azoaromatic polymer films. Appl Phys Lett 1995;66:136–8.
[69] Kim DY, Tripathy SK, Li L, Kumar J. Laser-induced holographic surface relief gratings on nonlinear optical polymer films. Appl Phys Lett 1995;66:1166–8.
[70] Yager KG, Barrett CJ. Temperature modeling of laser-irradiated azo-polymer thin films. J Chem Phys 2003;120:1089–96.
[71] Yager KG, Tanchak OM, Godbout C, Fritzsche H, Barrett CJ. Photomechanical effects in azo-polymers studied by neutron reflectometry. Macromolecules 2006;39:9311–9.
[72] Kim DY, Li L, Jiang XL, et al. Polarized laser induced holographic surface relief gratings on polymer films. Macromolecules 1995;28:8835–9.
[73] Ambrosio A, Camposeo A, Carella A, et al. Realization of submicrometer structures by a confocal system on azopolymer films containing photoluminescent chromophores. J Appl Phys 2010;107:083110.
[74] Jiang XL, Li L, Kumar J, Kim DY, Tripathy SK. Unusual polarization dependent optical erasure of surface relief gratings on azobenzene polymer films. Appl Phys Lett 1998;72:2502–4.
[75] Viswanathan NK, Kim DY, Bian S, et al. Surface relief structures on azo polymer films. J Mater Chem 1999;9:1941–55.
[76] Vapaavuori J, Ras RHA, Kaivola M, Bazuin CG, Priimagi A. From partial to complete optical erasure of azobenzene–polymer gratings: effect of molecular weight. J Mater Chem C 2015;3:11011–6.
[77] Natansohn A, Rochon P. Photoinduced motions in azobenzene-based amorphous polymers: possible photonic devices. Adv Mater 1999;11:1387–91.
[78] Cojocariu C, Rochon P. Light-induced motions in azobenzene-containing polymers. Pure Appl Chem 2009;76:1479–97.
[79] Lee S, Kang HS, Park J-K. Directional photofluidization lithography: micro/nanostructural evolution by photofluidic motions of azobenzene materials. Adv Mater 2012;24:2069–103.
[80] Priimagi A, Shevchenko A. Azopolymer-based micro- and nanopatterning for photonic applications. J Polym Sci Part B Polym Phys 2014;52:163–82.
[81] Lagugné Labarthet F, Buffeteau T, Sourisseau C. Analyses of the diffraction efficiencies, birefringence, and surface relief gratings on azobenzene-containing polymer films. J Phys Chem B 1998;102:2654–62.
[82] Laventure A, Bourotte J, Vapaavuori J, et al. Photoactive/passive molecular glass blends: an efficient strategy to optimize azomaterials for surface relief grating inscription. ACS Appl Mater Interfaces 2017;9:798–808.
[83] Goldenberg LM, Kulikovsky L, Kulikovska O, Stumpe J. Extremely high patterning efficiency in easily made azobenzene-containing polymer films. J Mater Chem 2009;19:6103–5.
[84] Zucolotto V, He J-A, Constantino CJL, et al. Mechanisms of surface-relief gratings formation in layer-by-layer films from azodyes. Polymer 2003;44:6129–33.
[85] Kulikovska O, Goldenberg LM, Stumpe J. Supramolecular azobenzene-based materials for optical generation of microstructures. Chem Mater 2007;19:3343–8.
[86] Priimagi A, Lindfors K, Kaivola M, Rochon P. Efficient surface-relief gratings in hydrogen-bonded polymer-azobenzene complexes. ACS Appl Mater Interfaces 2009;1:1183–9.
[87] Priimagi A, Cavallo G, Forni A, et al. Halogen bonding versus hydrogen bonding in driving self-assembly and performance of light-responsive supramolecular polymers. Adv Funct Mater 2012;22:2572–9.
[88] Priimagi A, Saccone M, Cavallo G, et al. Photoalignment and surface-relief-grating formation are efficiently combined in low-molecular-weight halogen-bonded complexes. Adv Mater 2012;24:OP345–52.

[89] Vapaavuori J, Geraldine Bazuin C, Priimagi A. Supramolecular design principles for efficient photoresponsive polymer–azobenzene complexes. J Mater Chem C 2018;6:2168–88.
[90] Nakano H, Takahashi T, Kadota T, Shirota Y. Formation of a surface relief grating using a novel azobenzene-based photochromic amorphous molecular material. Adv Mater 2002;14:1157–60.
[91] Guo M, Xu Z, Wang X. Photofabrication of two-dimensional quasi-crystal patterns on UV-curable molecular azo glass films. Langmuir 2008;24:2740–5.
[92] Ozols A, Reinfelde M, Saharov D, et al. Holographic recording of surface relief gratings in tolyle-based azobenzene oligomers. Thin Solid Films 2008;516:8887–92.
[93] Goldenberg LM, Kulikovsky L, Kulikovska O, Tomczyk J, Stumpe J. Thin layers of low molecular azobenzene materials with effective light-induced mass transport. Langmuir 2010;26:2214–7.
[94] Gharagozloo-Hubmann K, Kulikovska O, Börger V, Menzel H, Stumpe J. Surface relief gratings in azobenzene-containing polymers with linear and star-branched architectures: a comparison. Macromol Chem Phys 2009;210:1809–17.
[95] Vapaavuori J, Priimagi A, Soininen AJ, et al. Photoinduced surface patterning of azobenzene-containing supramolecular dendrons, dendrimers and dendronized polymers. Opt Mater Express 2013;3:711–22.
[96] Koskela JE, Liljeström V, Lim J, et al. Light-fuelled transport of large dendrimers and proteins. J Am Chem Soc 2014;136:6850–3.
[97] Ubukata T, Seki T, Ichimura K. Surface relief gratings in host–guest supramolecular materials. Adv Mater 2000;12:1675–8.
[98] Zettsu N, Seki T. Highly efficient photogeneration of surface relief structure and its immobilization in cross-linkable liquid crystalline azobenzene polymers. Macromolecules 2004;37:8692–8.
[99] Zettsu N, Ogasawara T, Arakawa R, et al. Highly photosensitive surface relief gratings formation in a liquid crystalline azobenzene polymer: new implications for the migration process. Macromolecules 2007;40:4607–13.
[100] Isayama J, Nagano S, Seki T. Phototriggered mass migrating motions in liquid crystalline azobenzene polymer films with systematically varied thermal properties. Macromolecules 2010;43:4105–12.
[101] Bian S, Li L, Kumar J, et al. Single laser beam-induced surface deformation on azobenzene polymer films. Appl Phys Lett 1998;73:1817–9.
[102] Yadavalli NS, Loebner S, Papke T, et al. A comparative study of photoinduced deformation in azobenzene containing polymer films. Soft Matter 2016;12:2593–603.
[103] Bian S, Williams JM, Kim DY, et al. Photoinduced surface deformations on azobenzene polymer films. J Appl Phys 1999;86:4498–508.
[104] Karageorgiev P, Neher D, Schulz B, et al. From anisotropic photo-fluidity towards nanomanipulation in the optical near-field. Nat Mater 2005;4:699.
[105] Chou SY, Xia Q. Improved nanofabrication through guided transient liquefaction. Nat Nanotechnol 2008;3:295–300.
[106] Wang Y, Liang X, Liang Y, Chou SY. Sub-10-nm wide trench, line, and hole fabrication using pressed self-perfection. Nano Lett 2008;8:1986–90.
[107] Mechau N, Saphiannikova M, Neher D. Dielectric and mechanical properties of azobenzene polymer layers under visible and ultraviolet irradiation. Macromolecules 2005;38:3894–902.
[108] Tanchak OM, Barrett CJ. Light-induced reversible volume changes in thin films of azo polymers: the photomechanical effect. Macromolecules 2005;38:10566–70.
[109] Yadavalli NS, Linde F, Kopyshev A, Santer S. Soft matter beats hard matter: rupturing of thin metallic films induced by mass transport in photosensitive polymer films. ACS Appl Mater Interfaces 2013;5:7743–7.
[110] Hurduc N, Donose B, Macovei A, et al. Direct observation of athermal photofluidisation in azo-polymer films. Soft Matter 2014;10:4640–7.
[111] Yadavalli NS, Korolkov D, Moulin J-F, Krutyeva M, Santer S. Probing opto-mechanical stresses within azobenzene-containing photosensitive polymer films by a thin metal film placed above. ACS Appl Mater Interfaces 2014;6:11333–40.
[112] Sorelli L, Fabbri F, Frech-Baronet J, et al. A closer look at the light-induced changes in the mechanical properties of azobenzene-containing polymers by statistical nanoindentation. J Mater Chem C 2015;3:11055–65.
[113] Hurduc N, Donose BC, Rocha L, Ibanescu C, Scutaru D. Azo-polymers photofluidisation – a transient state of matter emulated by molecular motors. RSC Adv 2016;6:27087–93.
[114] Sekhar Yadavalli N, Loebner S, Papke T, et al. A comparative study of photoinduced deformation in azobenzene containing polymer films. Soft Matter 2016;12:2593–603.
[115] Florio GD, Bründermann E, Yadavalli NS, Santer S, Havenith M. Confocal Raman microscopy and AFM study of the interface between the photosensitive polymer layer and multilayer graphene. Soft Mater 2014;12:S98–S105.
[116] Saphiannikova M, Toshchevikov V. Optical deformations of azobenzene polymers: Orientation approach vs. photofluidization concept. J Soc Inf Disp 2015;23:146–53.
[117] Fabbri F, Lassailly Y, Lahlil K, Boilot JP, Peretti J. Alternating photoinduced mass transport triggered by light polarization in azobenzene containing sol-gel films. Appl Phys Lett 2010;96:081908.
[118] Fabbri F, Garrot D, Lahlil K, et al. Evidence of two distinct mechanisms driving photoinduced matter motion in thin films containing azobenzene derivatives. J Phys Chem B 2011;115:1363–7.
[119] Fabbri F, Lassailly Y, Monaco S, et al. Kinetics of photoinduced matter transport driven by intensity and polarization in thin films containing azobenzene. Phys Rev B 2012;86:115440.
[120] Yadavalli NS, Santer S. In-situ atomic force microscopy study of the mechanism of surface relief grating formation in photosensitive polymer films. J Appl Phys 2013;113:224304.
[121] Yadavalli NS, Saphiannikova M, Lomadze N, Goldenberg LM, Santer S. Structuring of photosensitive material below diffraction limit using far field irradiation. Appl Phys A 2013;113:263–72.
[122] Yadavalli NS, Saphiannikova M, Santer S. Photosensitive response of azobenzene containing films towards pure intensity or polarization interference patterns. Appl Phys Lett 2014;105:051601.
[123] Yadavalli NS, König T, Santer S. Selective mass transport of azobenzene-containing photosensitive films towards or away from the light intensity. J Soc Inf Disp 2015;23:154–62.

[124] Naydenova I, Nikolova L, Todorov T, et al. Diffraction from polarization holographic gratings with surface relief in side-chain azobenzene polyesters. JOSA B 1998;15:1257–65.
[125] Labarthet FL, Buffeteau T, Sourisseau C. Time dependent analysis of the formation of a half-period surface relief grating on amorphous azopolymer films. J Appl Phys 2001;90:3149–58.
[126] Sobolewska A, Miniewicz A. On the inscription of period and half-period surface relief gratings in azobenzene-functionalized polymers. J Phys Chem B 2008;112:4526–35.
[127] Hubert C, Fiorini-Debuisschert C, Maurin I, Nunzi J-M, Raimond P. Spontaneous patterning of hexagonal structures in an azo-polymer using light-controlled mass transport. Adv Mater 2002;14:729–32.
[128] Tsutsumi N, Fujihara A. Pulsed laser induced spontaneous gratings on a surface of azobenzene polymer. Appl Phys Lett 2004;85:4582–4.
[129] Hubert C, Fiorini-Debuisschert C, Hassiaoui I, et al. Emission properties of an organic light-emitting diode patterned by a photoinduced autostructuration process. Appl Phys Lett 2005;87:191105.
[130] Barille R, Nunzi J-M, Ahmadi-Kandjani S, Ortyl E, Kucharski S. One step inscription of surface relief micrograting. Opt Commun 2007;280:217–20.
[131] Hubert C, Fiorini-Debuisschert C, Rocha L, Raimond P, Nunzi J-M. Spontaneous photoinduced patterning of azo-dye polymer films: the facts. JOSA B 2007;24:1839–46.
[132] Lee S, Jeong Y-C, Park J-K. Unusual surface reliefs from photoinduced creeping and aggregation behavior of azopolymer. Appl Phys Lett 2008;93:031912.
[133] Leblond H, Barille R, Ahmadi-Kandjani S, et al. Spontaneous formation of optically induced surface relief gratings. J Phys B At Mol Opt Phys 2009;42:205401.
[134] Yin J, Ye G, Wang X. Self-structured surface patterns on molecular azo glass films induced by laser light irradiation. Langmuir 2010;26:6755–61.
[135] Ambrosio A, Maddalena P, Carella A, et al. Two-photon induced self-structuring of polymeric films based on Y-shape azobenzene chromophore. J Phys Chem C 2011;115:13566–70.
[136] Wang X, Yin J, Wang X. Self-structured surface patterns on epoxy-based azo polymer films induced by laser light irradiation. Macromolecules 2011;44:6856–67.
[137] Wang X, Yin J, Wang X. Photoinduced self-structured surface pattern on a molecular azo glass film: structure–property relationship and wavelength correlation. Langmuir 2011;27:12666–76.
[138] Ambrosio A, Girardo S, Camposeo A, Pisignano D, Maddalena P. Controlling spontaneous surface structuring of azobenzene-containing polymers for large-scale nano-lithography of functional substrates. Appl Phys Lett 2013;102:093102.
[139] Mazaheri L, Ahmadi-Kandjani S, Nunzi J-M. Influence of temperature on the relaxation kinetics of spontaneous pattern formation in an azo-polymer film. Opt Commun 2013;298:150–3.
[140] Galinski H, Ambrosio A, Maddalena P, et al. Instability-induced pattern formation of photoactivated functional polymers. Proc Natl Acad Sci 2014;111:17017–22.
[141] Sobolewska A, Bartkiewicz S. Single beam test (SBT) as a criterion for the resolution of holographic recording. J Mater Chem C 2015;3:5616–20.
[142] Teboul V, Barillé R, Tajalli P, et al. Light mediated emergence of surface patterns in azopolymers at low temperatures. Soft Matter 2015;11:6444–9.
[143] Mazaheri L, Bobbara SR, Lebel O, Nunzi J-M. Photoinduction of spontaneous surface relief gratings on Azo DR1 glass. Opt Lett 2016;41:2958–61.
[144] Mazaheri L, Sabat RG, Lebel O, Nunzi J-M. Unraveling the nucleation and growth of spontaneous surface relief gratings. Opt Mater 2016;62:378–91.
[145] Noga J, Sobolewska A, Bartkiewicz S, Virkki M, Priimagi A. Periodic surface structures induced by a single laser beam irradiation. Macromol Mater Eng 2017;302:1600329.
[146] Siegman A, Fauchet P. Stimulated Wood's anomalies on laser-illuminated surfaces. IEEE J Quantum Electron 1986;22:1384–403.
[147] Bolle M, Lazare S. Characterization of submicrometer periodic structures produced on polymer surfaces with low-fluence ultraviolet laser radiation. J Appl Phys 1993;73:3516–24.
[148] Nivas JJ, Gesuele F, Allahyari E, et al. Effects of ambient air pressure on surface structures produced by ultrashort laser pulse irradiation. Opt Lett 2017;42:2710–3.
[149] Ambrosio A, Marrucci L, Borbone F, Roviello A, Maddalena P. Light-induced spiral mass transport in azo-polymer films under vortex-beam illumination. Nat Commun 2012;3:989.
[150] Ambrosio A, Maddalena P, Marrucci L. Molecular model for light-driven spiral mass transport in azopolymer films. Phys Rev Lett 2013;110:146102.
[151] Marrucci L, Manzo C, Paparo D. Optical spin-to-orbital angular momentum conversion in inhomogeneous anisotropic media. Phys Rev Lett 2006;96:163905.
[152] Franke-Arnold S, Allen L, Padgett M. Advances in optical angular momentum. Laser Photonics Rev 2008;2:299–313.
[153] Devlin R C, Ambrosio A, Wintz D, et al. Spin-to-orbital angular momentum conversion in dielectric metasurfaces. Opt Express 2017;25:377–93.
[154] Devlin RC, Ambrosio A, Rubin NA, Mueller JPB, Capasso F. Arbitrary spin-to-orbital angular momentum conversion of light. Science 2017;358:896–901.
[155] Barrett CJ, Rochon PL, Natansohn AL. Model of laser-driven mass transport in thin films of dye-functionalized polymers. J Chem Phys 1998;109:1505–16.
[156] Bublitz D, Fleck B, Wenke L. A model for surface-relief formation in azobenzene polymers. Appl Phys B 2001;72:931–6.
[157] Toshchevikov V, Saphiannikova M, Heinrich G. Microscopic theory of light-induced deformation in amorphous side-chain azobenzene polymers. J Phys Chem B 2009;113:5032–45.
[158] Toshchevikov V, Ilnytskyi J, Saphiannikova M. Photoisomerization kinetics and mechanical stress in azobenzene-containing materials. J Phys Chem Lett 2017;8:1094–8.
[159] Kumar J, Li L, Jiang XL, et al. Gradient force: the mechanism for surface relief grating formation in azobenzene functionalized polymers. Appl Phys Lett 1998;72:2096–8.
[160] Sumaru K, Fukuda T, Kimura T, Matsuda H, Yamanaka T. Photoinduced surface relief formation on azopolymer films: a driving force and formed relief profile. J Appl Phys 2002;91:3421–30.
[161] Yang K, Yang S, Kumar J. Formation mechanism of surface relief structures on amorphous azopolymer films. Phys Rev B 2006;73:165204.

[162] Lefin P, Fiorini C, Nunzi J-M. Anisotropy of the photo-induced translation diffusion of azobenzene dyes in polymer matrices. Pure Appl Opt J Eur Opt Soc Part A 1998;7:71.
[163] Fiorini C, Prudhomme N, de Veyrac G, et al. Molecular migration mechanism for laser induced surface relief grating formation. Synth Met 2000;115:121–5.
[164] Juan ML, Plain J, Bachelot R, et al. Multiscale model for photoinduced molecular motion in azo polymers. ACS Nano 2009;3:1573–9.
[165] Sobolewska A, Bartkiewicz S. Surface relief grating in azo-polymer obtained for s-s polarization configuration of the writing beams. Appl Phys Lett 2012;101:193301.
[166] Sobolewska A, Bartkiewicz S, Priimagi A. High-modulation-depth surface relief gratings using s–s polarization configuration in supramolecular polymer-azobenzene complexes. J Phys Chem C 2014;118:23279–84.
[167] Rahmouni A, Bougdid Y, Moujdi S, Nesterenko DV, Sekkat Z. Photoassisted holography in azo dye doped polymer films. J Phys Chem B 2016;120:11317–22.
[168] Gritsai Y, Goldenberg LM, Stumpe J. Efficient single-beam light manipulation of 3D microstructures in azobenzene-containing materials. Opt Express 2011;19:18687–95.
[169] Yager KG, Barrett CJ. All-optical patterning of azo polymer films. Curr Opin Solid State Mater Sci 2001;5:487–94.
[170] Ilnytskyi JM, Neher D, Saphiannikova M. Opposite photo-induced deformations in azobenzene-containing polymers with different molecular architecture: molecular dynamics study. J Chem Phys 2011;135:044901.
[171] Watabe M, Juman G, Miyamoto K, Omatsu T. Light induced conch-shaped relief in an azo-polymer film. Sci Rep 2014;4:srep04281.
[172] Barada D, Fukuda T, Itoh M, Yatagai T. Numerical analysis of photoinduced surface relief grating formation by particle method. Opt Rev 2005;12:271–3.
[173] Ishitobi H, Nakamura I, Kobayashi T, et al. Nanomovement of azo polymers induced by longitudinal fields. ACS Photonics 2014;1:190–7.
[174] Ishitobi H, Tanabe M, Sekkat Z, Kawata S. Nanomovement of azo polymers induced by metal tip enhanced near-field irradiation. Appl Phys Lett 2007;91:091911.
[175] Grosjean T, Courjon D. Photopolymers as vectorial sensors of the electric field. Opt Express 2006;14:2203–10.
[176] Gilbert Y, Bachelot R, Royer P, et al. Longitudinal anisotropy of the photoinduced molecular migration in azobenzene polymer films. Opt Lett 2006;31:613–5.
[177] Ambrosio A, Camposeo A, Maddalena P, Patanè S, Allegrini M. Real-time monitoring of the surface relief formation on azo-polymer films upon near-field excitation. J Microsc 2008;229:307–12.
[178] Lee S, Kang H S, Ambrosio A, Park J-K, Marrucci L. Directional superficial photofluidization for deterministic shaping of complex 3D architectures. ACS Appl Mater Interfaces 2015;7:8209–17.
[179] Plain J, Wiederrecht GP, Gray SK, Royer P, Bachelot R. Multi-scale optical imaging of complex fields based on the use of azobenzene nanomotors. J Phys Chem Lett 2013;4:2124–32.
[180] Pohl DW. Optical stethoscopy: image recording with resolution $\lambda/20$. Appl Phys Lett 1984;44:651–3.
[181] Betzig E, Lewis A, Harootunian A, Isaacson M, Kratschmer E. Near field scanning optical microscopy (NSOM). Biophys J 1986;49:269–79.
[182] Ambrosio A, Alderighi M, Labardi M, et al. Near-field optical microscopy of polymer-based films with dispersed terthiophene chromophores for polarizer applications. Nanotechnology 2004;15:S270.
[183] Ambrosio A, Allegrini M, Latini G, Cacialli F. Thermal processes in metal-coated fiber probes for near-field experiments. Appl Phys Lett 2005;87:033109.
[184] Ambrosio A, Cefalì E, Spadaro S, et al. Noncontact tuning fork position sensing for hollow-pyramid near-field cantilevered probes. Appl Phys Lett 2006;89:163108.
[185] Bachelot R, H'Dhili F, Barchiesi D, et al. Apertureless near-field optical microscopy: a study of the local tip field enhancement using photosensitive azobenzene-containing films. J Appl Phys 2003;94:2060–72.
[186] Patanè S, Arena A, Allegrini M, et al. Near-field optical writing on azo-polymethacrylate spin-coated films. Opt Commun 2002;210:37–41.
[187] Hubert C, Rumyantseva A, Lerondel G, et al. Near-field photochemical imaging of noble metal nanostructures. Nano Lett 2005;5:615–9.
[188] Hubert C, Bachelot R, Plain J, et al. Near-field polarization effects in molecular-motion-induced photochemical imaging. J Phys Chem C 2008;112:4111–6.
[189] Derouard M, Hazart J, Lérondel G, et al. Polarization-sensitive printing of surface plasmon interferences. Opt Express 2007;15:4238–46.
[190] König T, Santer S. Stretching and distortion of a photosensitive polymer film by surface plasmon generated near fields in the vicinity of a nanometer sized metal pin hole. Nanotechnology 2012;23:155301.
[191] Papke T, Yadavalli NS, Henkel C, Santer S. Mapping a plasmonic hologram with photosensitive polymer films: standing versus propagating waves. ACS Appl Mater Interfaces 2014;6:14174–80.
[192] Lee S, Jeong Y-C, Park J-K. Facile fabrication of close-packed microlens arrays using photoinduced surface relief structures as templates. Opt Express 2007;15:14550–9.
[193] Jeong SM, Araoka F, Machida Y, et al. Enhancement of light extraction from organic light-emitting diodes with two-dimensional hexagonally nanoimprinted periodic structures using sequential surface relief grating. Jpn J Appl Phys 2008;47:4566.
[194] Wang J, Wang X, He Y. Fabrication of fluorescent surface relief patterns using AIE polymer through a soft lithographic approach. J Polym Sci Part B Polym Phys 2016;54:1838–45.
[195] Cooper SR, Tomkins DW, Petty M. Surface-relief diffraction gratings recorded by multiple-beam coherent phase exposure. Opt Lett 1997;22:357–9.
[196] Emoto A, Ono H, Kawatsuki N, Uchida E. Two-dimensional anisotropic gratings formed in photocrosslinkable polymer liquid crystals by multiple interference. Jpn J Appl Phys 2006;45:1705.
[197] Wu X, Ngan Nguyen TT, Ledoux-Rak I, Thanh Nguyen C, Diep N. Optically accelerated formation of one- and two-dimensional holographic surface relief gratings on DR1/PMMA in holography. In: Mihaylova E., ed. Basic principles and contemporary applications. Rijeka, Croatia, InTech, 2013. DOI: 10.5772/53788.
[198] Tofini A, Levesque L, Lebel O, Georges Sabat R. Erasure of surface relief gratings in azobenzene molecular glasses by localized heating using a CO_2 laser. J Mater Chem C 2018;6:1083–91.

[199] Zhao Y, Lu Q, Li M, Li X. Anisotropic wetting characteristics on submicrometer-scale periodic grooved surface. Langmuir 2007;23:6212–7.
[200] Chen Y, He B, Lee J, Patankar NA. Anisotropy in the wetting of rough surfaces. J Colloid Interface Sci 2005;281:458–64.
[201] Kusumaatmaja H, Vrancken RJ, Bastiaansen CWM, Yeomans JM. Anisotropic drop morphologies on corrugated surfaces. Langmuir 2008;24:7299–308.
[202] Rianna C, Calabuig A, Ventre M, et al. Reversible holographic patterns on azopolymers for guiding cell adhesion and orientation. ACS Appl Mater Interfaces 2015;7:16984–91.
[203] Li W, Fang G, Li Y, Qiao G. Anisotropic wetting behavior arising from superhydrophobic surfaces: parallel grooved structure. J Phys Chem B 2008;112:7234–43.
[204] Hancock MJ, Sekeroglu K, Demirel MC. Bioinspired directional surfaces for adhesion, wetting, and transport. Adv Funct Mater 2012;22:2223–4.
[205] Baac H, Lee J-H, Seo J-M, et al. Submicron-scale topographical control of cell growth using holographic surface relief grating. Mater Sci Eng C 2004;24:209–12.
[206] Barillé R, Janik R, Kucharski S, Eyer J, Letournel F. Photoresponsive polymer with erasable and reconfigurable micro- and nano-patterns: an in vitro study for neuron guidance. Colloids Surf B Biointerfaces 2011;88:63–71.
[207] Hurduc N, Macovei A, Paius C, et al. Azo-polysiloxanes as new supports for cell cultures. Mater Sci Eng C 2013;33:2440–5.
[208] Rocha L, Păiuş C-M, Luca-Raicu A, et al. Azobenzene based polymers as photoactive supports and micellar structures for applications in biology. J Photochem Photobiol Chem 2014;291:16–25.
[209] Rianna C, Rossano L, Kollarigowda RH, et al. Spatio-temporal control of dynamic topographic patterns on azopolymers for cell culture applications. Adv Funct Mater 2016;26:7572–80.
[210] Fedele C, De Gregorio M, Netti PA, Cavalli S, Attanasio C. Azopolymer photopatterning for directional control of angiogenesis. Acta Biomater 2017;63:317–25.
[211] Fedele C, Netti P, Cavalli S. Azobenzene-based polymers: emerging applications as cell culture platforms. Biomater Sci 2018;6:990–5.
[212] Flemming RG, Murphy CJ, Abrams GA, Goodman SL, Nealey PF. Effects of synthetic micro- and nano-structured surfaces on cell behavior. Biomaterials 1999;20:573–88.
[213] Bettinger CJ, Langer R, Borenstein JT. Engineering substrate micro- and nanotopography to control cell function. Angew Chem Int Ed Engl 2009;48:5406–15.
[214] Goldenberg LM, Gritsai Y, Kulikovska O, Stumpe J. Three-dimensional planarized diffraction structures based on surface relief gratings in azobenzene materials. Opt Lett 2008;33:1309–11.
[215] Gritsai Y, Goldenberg LM, Kulikovska O, Stumpe J. 3D structures using surface relief gratings of azobenzene materials. J Opt Pure Appl Opt 2008;10:125304.
[216] Goldenberg LM, Kulikovsky L, Kulikovska O, Stumpe J. New materials with detachable azobenzene: effective, colourless and extremely stable surface relief gratings. J Mater Chem 2009;19:8068–71.
[217] Goldenberg LM, Kulikovsky L, Gritsai Y, et al. Very efficient surface relief holographic materials based on azobenzene -containing epoxy resins cured in films. J Mater Chem 2010;20:9161–71.
[218] Paterson J, Natansohn A, Rochon P, Callender CL, Robitaille L. Optically inscribed surface relief diffraction gratings on azobenzene-containing polymers for coupling light into slab waveguides. Appl Phys Lett 1996;69:3318–20.
[219] Rochon P, Natansohn A, Callender CL, Robitaille L. Guided mode resonance filters using polymer films. Appl Phys Lett 1997;71:1008–10.
[220] Stockermans RJ, Rochon PL. Narrow-band resonant grating waveguide filters constructed with azobenzene polymers. Appl Opt 1999;38:3714–9.
[221] Kang J-W, Kim M-J, Kim J-P, et al. Polymeric wavelength filters fabricated using holographic surface relief gratings on azobenzene-containing polymer films. Appl Phys Lett 2003;82:3823–5.
[222] Lausten R, Rochon P, Ivanov M, et al. Optically reconfigurable azobenzene polymer-based fiber Bragg filter. Appl Opt 2005;44:7039–42.
[223] Perschke A, Fuhrmann T. Molecular azo glasses as grating couplers and resonators for optical devices. Adv Mater 2002;14:841–3.
[224] Golghasemi Sorkhabi S, Ahmadi-Kandjani S, Cousseau F, et al. Surface quasi periodic and random structures based on nanomotor lithography for light trapping. J Appl Phys 2017;122:015303.
[225] Goldenberg LM, Lisinetskii V, Gritsai Y, Stumpe J, Schrader S. Single step optical fabrication of a DFB laser device in fluorescent azobenzene-containing materials. Adv Mater 2012;24:3339–43.
[226] Kim S-S, Chun C, Hong J-C, Kim D-Y. Well-ordered TiO 2 nanostructures fabricated using surface relief gratings on polymer films. J Mater Chem 2006;16:370–5.
[227] Alasaarela T, Zheng D, Huang L, et al. Single-layer one-dimensional nonpolarizing guided-mode resonance filters under normal incidence. Opt Lett 2011;36:2411–3.
[228] Kogelnik H, Shank CV. Coupled-wave theory of distributed feedback lasers. J Appl Phys 1972;43:2327.
[229] Ghafouri-Shiraz H. Principles of distributed feedback semiconductor laser diodes: coupled wave theory. In: Ghafouri-Shiraz H., ed. Distributed Feedback Laser Diodes and Optical Tunable Filters. Hoboken, NJ, USA, John Wiley & Sons, Ltd., 2003, 31–78. DOI: 10.1002/0470856238.ch2.
[230] Rocha L, Dumarcher V, Denis C, et al. Laser emission in periodically modulated polymer films. J Appl Phys 2001;89:3067–9.
[231] Ubukata T, Isoshima T, Hara M. Wavelength-programmable organic distributed-feedback laser based on a photoassisted polymer-migration system. Adv Mater 2005;17:1630–3.
[232] Goldenberg LM, Lisinetskii V, Gritsai Y, Stumpe J, Schrader S. Second order DFB lasing using reusable grating inscribed in azobenzene-containing material. Opt Mater Express 2012;2:11–9.
[233] Goldenberg LM, Lisinetskii V, Gritsai Y, Stumpe J, Schrader S. First observation of DFB lasing in polarization gratings written in azobenzene film. Laser Phys Lett 2013;10:085804.
[234] Goldenberg LM, Lisinetskii VA, Schrader S. Continuously tunable laser based on polarization gratings in azobenzene-containing material. Laser Phys 2014;24:035807.
[235] Goldenberg LM, Lisinetskii V, Ryabchun A, Bobrovsky A, Schrader S. Influence of the cation type on the DFB lasing performance of dye-doped azobenzene-containing polyelectrolytes. J Mater Chem C 2014;2:8546–53.
[236] Goldenberg LM, Lisinetskii V, Ryabchun A, Bobrovsky A, Schrader S. Liquid crystalline azobenzene-containing polymer

as a matrix for distributed feedback lasers. ACS Photonics 2014;1:885–93.
[237] Novitsky DV, Katarkevich VM, Efendiev TS. Dynamics of DFB dye lasing by polarization modulation: simulations and experiment. Laser Phys Lett 2016;13:025002.
[238] Parafiniuk K, Monnereau C, Sznitko L, et al. Distributed feedback lasing in amorphous polymers with covalently bonded fluorescent dyes: the influence of photoisomerization process. Macromolecules 2017;50:6164–73.
[239] Garnett E, Yang P. Light trapping in silicon nanowire solar cells. Nano Lett 2010;10:1082–7.
[240] Hu Z, Zhang J, Zhao Y. Effect of textured electrodes with light-trapping on performance of polymer solar cells. J Appl Phys 2012;111:104516.
[241] Windisch R, Heremans P, Knobloch A, et al. Light-emitting diodes with 31% external quantum efficiency by outcoupling of lateral waveguide modes. Appl Phys Lett 1999;74:2256.
[242] Koo WH, Jeong SM, Araoka F, et al. Light extraction from organic light-emitting diodes enhanced by spontaneously formed buckles. Nat Photonics 2010;4:222.
[243] Zhou L, Jiang X, Li Y, et al. Light extraction of trapped optical modes in polymer light-emitting diodes with nanoimprinted double-pattern gratings. ACS Appl Mater Interfaces 2014;6:18139–46.
[244] Ramanujam PS, Pedersen M, Hvilsted S. Instant holography. Appl Phys Lett 1999;74:3227–9.
[245] Harada K, Itoh M, Yatagai T, Kamemaru S. Application of surface relief hologram using azobenzene containing polymer film. Opt Rev 2005;12:130–4.
[246] Lee LP, Szema R. Inspirations from biological optics for advanced photonic systems. Science 2005;310:1148–50.
[247] Park JH, Park KJ, Jiang T, et al. Light-transformable and -healable triboelectric nanogenerators. Nano Energy 2017;38:412–8.
[248] Xia Y, Kim E, Zhao X-M, et al. Complex optical surfaces formed by replica molding against elastomeric masters. Science 1996;273:347–9.
[249] Xia Y, Whitesides GM. Soft lithography. Angew Chem Int Ed 1998;37:550–75.
[250] Guo LJ. Nanoimprint lithography: methods and material requirements. Adv Mater 2007;19:495–513.
[251] Qin D, Xia Y, Whitesides GM. Soft lithography for micro- and nanoscale patterning. Nat Protoc 2010;5:491–502.
[252] Liu B, Wang M, He Y, Wang X. Duplication of photoinduced azo polymer surface-relief gratings through a soft lithographic approach. Langmuir 2006;22:7405–10.
[253] Matsui T, Ozaki M, Yoshino K, Kajzar F. Fabrication of flexible distributed feedback laser using photoinduced surface relief grating on azo-polymer film as a template. Jpn J Appl Phys 2002;41:L1386.
[254] Cocoyer C, Rocha L, Fiorini-Debuisschert C, et al. Implementation of a submicrometer patterning technique in azopolymer films towards optimization of photovoltaic solar cells efficiency. Thin Solid Films 2006;511–512:517–22.
[255] Cocoyer C, Rocha L, Sicot L, et al. Implementation of submicrometric periodic surface structures toward improvement of organic-solar-cell performances. Appl Phys Lett 2006;88:133108.
[256] Na S-I, Kim S-S, Kwon S-S, et al. Surface relief gratings on poly(3-hexylthiophene) and fullerene blends for efficient organic solar cells. Appl Phys Lett 2007;91:173509.
[257] Na S-I, Kim S-S, Jo J, et al. Efficient polymer solar cells with surface relief gratings fabricated by simple soft lithography. Adv Funct Mater 2008;18:3956–63.
[258] Kim J, Park H, Na S-I, Noh Y-Y, Kim D-Y. A facile approach to improve light extraction for organic light emitting diodes via azobenzene surface relief gratings. Jpn J Appl Phys 2014;53:08NF02.
[259] Yang S, Yang K, Niu L, et al. Patterning of substrates using surface relief structures on an azobenzene-functionalized polymer film. Adv Mater 2004;16:693–6.
[260] Kravchenko A, Shevchenko A, Ovchinnikov V, Priimagi A, Kaivola M. Optical interference lithography using azobenzene-functionalized polymers for micro- and nanopatterning of silicon. Adv Mater 2011;23:4174–7.
[261] Kravchenko A, Shevchenko A, Ovchinnikov V, Grahn P, Kaivola M. Fabrication and characterization of a large-area metal nano-grid wave plate. Appl Phys Lett 2013;103:033111.
[262] Kravchenko A, Shevchenko A, Grahn P, Ovchinnikov V, Kaivola M. Photolithographic periodic patterning of gold using azobenzene-functionalized polymers. Thin Solid Films 2013;540:162–7.
[263] Moerland RJ, Koskela JE, Kravchenko A, et al. Large-area arrays of three-dimensional plasmonic subwavelength-sized structures from azopolymer surface-relief gratings. Mater Horiz 2013;1:74–80.
[264] Horstmeyer R, Heintzmann R, Popescu G, Waller L, Yang C. Standardizing the resolution claims for coherent microscopy. Nat Photonics 2016;10:68–71.
[265] Oscurato SL, Borbone F, Devlin RC, et al. New microscopy technique based on position localization of scattering particles. Opt Express 2017;25:11530–49.
[266] Kang HS, Lee S, Park J-K. Monolithic, hierarchical surface reliefs by holographic photofluidization of azopolymer arrays: direct visualization of polymeric flows. Adv Funct Mater 2011;21:4412–22.
[267] Oscurato SL, Borbone F, Maddalena P, Ambrosio A. Light-driven wettability tailoring of azopolymer surfaces with reconfigured three-dimensional posts. ACS Appl Mater Interfaces 2017;9:30133–42.
[268] Lambeth RH, Park J, Liao H, et al. Proximity field nanopatterning of azopolymer thin films. Nanotechnology 2010;21:165301.
[269] Choi J, Cho W, Jung YS, Kang HS, Kim H-T. Direct fabrication of micro/nano-patterned surfaces by vertical-directional photofluidization of azobenzene materials. ACS Nano 2017;11:1320–7.
[270] Kang HS, Lee S, Lee S-A, Park J-K. Multi-level micro/nanotexturing by three-dimensionally controlled photofluidization and its use in plasmonic applications. Adv Mater 2013;25:5490–7.
[271] Pirani F, Angelini A, Frascella F, et al. Light-driven reversible shaping of individual azopolymeric micro-pillars. Sci Rep 2016;6:31702.
[272] Lee S, Shin J, Lee Y-H, Fan S, Park J-K. Directional photofluidization lithography for nanoarchitectures with controlled shapes and sizes. Nano Lett 2010;10:296–304.
[273] Lee S, Kang HS, Park J-K. High-resolution patterning of various large-area, highly ordered structural motifs by directional photofluidization lithography: sub-30-nm line,

ellipsoid, rectangle, and circle arrays. Adv Funct Mater 2011;21:1770–8.
[274] Dubrovkin AM, Barillé R, Ortyl E, Zielinska S. Photoinduced doughnut-shaped nanostructures. Chem Phys Lett 2014;599:7–11.
[275] Dubrovkin AM, Barillé R, Ortyl E, Zielinska S. Near-field optical control of doughnut-shaped nanostructures. Opt Commun 2015;334:147–51.
[276] Wang W, Du C, Wang X, et al. Directional photomanipulation of breath figure arrays. Angew Chem Int Ed 2014;53:12116–9.
[277] Sorkhabi SG, Barille R, Ahmadi-Kandjani S, Zielinska S, Ortyl E. A new method for patterning azopolymer thin film surfaces. Opt Mater 2017;66:573–9.
[278] Wang W, Yao Y, Luo T, et al. Deterministic reshaping of breath figure arrays by directional photomanipulation. ACS Appl Mater Interfaces 2017;9:4223–30.
[279] Wang W, Gao F, Yao Y, Lin S-L. Directional photo-manipulation of self-assembly patterned microstructures. Chin J Polym Sci 2018;36:297–305.
[280] Liu B, He Y, Fan P, Wang X. Azo polymer microspherical cap array: soft-lithographic fabrication and photoinduced shape deformation behavior. Langmuir 2007;23:11266–72.
[281] Kong X, Wang X, Luo T, et al. Photomanipulated architecture and patterning of azopolymer array. ACS Appl Mater Interfaces 2017;9:19345–53.
[282] Li Y, He Y, Tong X, Wang X. Photoinduced deformation of amphiphilic azo polymer colloidal spheres. J Am Chem Soc 2005;127:2402–3.
[283] Li J, Chen L, Xu J, et al. Photoguided shape deformation of azobenzene-containing polymer microparticles. Langmuir 2015;31:13094–100.
[284] Zhou X, Du Y, Wang X. Azo polymer janus particles and their photoinduced, symmetry-breaking deformation. ACS Macro Lett 2016;5:234–7.
[285] Loebner S, Lomadze N, Kopyshev A, et al. Light-induced deformation of azobenzene-containing colloidal spheres: calculation and measurement of opto-mechanical stresses. J Phys Chem B 2018;122:2001–9.
[286] Feng L, Li S, Li Y, et al. Super-hydrophobic surfaces: from natural to artificial. Adv Mater 2002;14:1857–60.
[287] Sun T, Feng L, Gao X, Jiang L. Bioinspired surfaces with special wettability. Acc Chem Res 2005;38:644–52.
[288] Blossey R. Self-cleaning surfaces – virtual realities. Nat Mater 2003;2:301–6.
[289] Tuteja A, Choi W, Ma M, et al. Designing superoleophobic surfaces. Science 2007;318:1618–22.
[290] Tuteja A, Choi W, Mabry JM, McKinley GH, Cohen RE. Robust omniphobic surfaces. Proc Natl Acad Sci 2008;105:18200–5.
[291] Cao L, Hu H-H, Gao D. Design and fabrication of micro-textures for inducing a superhydrophobic behavior on hydrophilic materials. Langmuir 2007;23:4310–4.
[292] Hensel R, Helbig R, Aland S, et al. Tunable nano-replication to explore the omniphobic characteristics of springtail skin. NPG Asia Mater 2013;5:e37.
[293] Liu T, Kim C-J. Turning a surface superrepellent even to completely wetting liquids. Science 2014;346:1096–100.
[294] Choi J, Jo W, Lee SY, et al. Flexible and robust superomniphobic surfaces created by localized photofluidization of azopolymer pillars. ACS Nano 2017;11:7821–8.
[295] Pirani F, Angelini A, Ricciardi S, Frascella F, Descrovi E. Laser-induced anisotropic wettability on azopolymeric micro-structures. Appl Phys Lett 2017;110:101603.
[296] Armani DK, Kippenberg TJ, Spillane SM, Vahala KJ. Ultra-high-Q toroid microcavity on a chip. Nature 2003;421:925–8.
[297] Eikema KSE. Frequency combs: liberated from material dispersion. Nat Photonics 2011;5:258–60.
[298] Park KJ, Park JH, Huh J-H, et al. Petal-inspired diffractive grating on a wavy surface: deterministic fabrications and applications to colorizations and LED devices. ACS Appl Mater Interfaces 2017;9:9935–44.
[299] Lee S-A, Kang HS, Park J-K, Lee S. Vertically oriented, three-dimensionally tapered deep-subwavelength metallic nanohole arrays developed by photofluidization lithography. Adv Mater 2014;26:7521–8.
[300] Nie S, Emory SR. Probing single molecules and single nanoparticles by surface-enhanced Raman scattering. Science 1997;275:1102–6.
[301] Huang KCY, Seo M-K, Sarmiento T, et al. Electrically driven subwavelength optical nanocircuits. Nat Photonics 2014;8:244–9.
[302] De Gennes P-G, Hébert M, Kant R. Artificial muscles based on nematic gels. Macromol Symp 1997;113:39–49.
[303] Finkelmann H, Nishikawa E, Pereira GG, Warner M. A new opto-mechanical effect in solids. Phys Rev Lett 2001;87:015501.
[304] Li M-H, Keller P, Li B, Wang X, Brunet M. Light-driven side-on nematic elastomer actuators. Adv Mater 2003;15:569–72.
[305] Barrett CJ, Mamiya J, Yager KG, Ikeda T. Photo-mechanical effects in azobenzene-containing soft materials. Soft Matter 2007;3:1249–61.
[306] Ikeda T, Mamiya J, Yu Y. Photomechanics of liquid-crystalline elastomers and other polymers. Angew Chem Int Ed 2007;46:506–28.
[307] Ohm C, Brehmer M, Zentel R. Liquid crystalline elastomers as actuators and sensors. Adv Mater 2010;22:3366–87.
[308] Mahimwalla Z, Yager KG, Mamiya J, et al. Azobenzene photomechanics: prospects and potential applications. Polym Bull 2012;69:967–1006.
[309] White TJ, Broer DJ. Programmable and adaptive mechanics with liquid crystal polymer networks and elastomers. Nat Mater 2015;14:1087–98.
[310] Shahsavan H, Yu L, Jákli A, Zhao B. Smart biomimetic micro/nanostructures based on liquid crystal elastomers and networks. Soft Matter 2017;13:8006–22.
[311] Kowalski BA, Guin TC, Auguste AD, Godman NP, White TJ. Pixelated polymers: directed self assembly of liquid crystalline polymer networks. ACS Macro Lett 2017;6:436–41.
[312] Ikeda T, Nakano M, Yu Y, Tsutsumi O, Kanazawa A. Anisotropic bending and unbending behavior of azobenzene liquid-crystalline gels by light exposure. Adv Mater 2003;15:201–5.
[313] Yu Y, Nakano M, Shishido A, Shiono T, Ikeda T. Effect of cross-linking density on photoinduced bending behavior of oriented liquid-crystalline network films containing azobenzene. Chem Mater 2004;16:1637–43.
[314] Camacho-Lopez M, Finkelmann H, Palffy-Muhoray P, Shelley M. Fast liquid-crystal elastomer swims into the dark. Nat Mater 2004;3:nmat1118.
[315] Yu Y, Nakano M, Maeda T, Kondo M, Ikeda T. Precisely direction-controllable bending of cross-linked liquid-crystal-

line polymer films by light. Mol Cryst Liq Cryst 2005;436:281/[1235]–290/[1244].
[316] Oosten CL van, Harris KD, Bastiaansen CWM, Broer DJ. Glassy photomechanical liquid-crystal network actuators for microscale devices. Eur Phys JE 2007;23:329–36.
[317] Mol GN, Harris KD, Bastiaansen CWM, Broer DJ. Thermomechanical responses of liquid-crystal networks with a splayed molecular organization. Adv Funct Mater 2005;15:1155–9.
[318] Kondo M, Yu Y, Ikeda T. How does the initial alignment of mesogens affect the photoinduced bending behavior of liquid-crystalline elastomers? Angew Chem Int Ed 2006;45:1378–82.
[319] Rogóż M, Zeng H, Xuan C, Wiersma DS, Wasylczyk P. Light-driven soft robot mimics caterpillar locomotion in natural scale. Adv Opt Mater 2016;4:1689–94.
[320] Iamsaard S, Aßhoff SJ, Matt B, et al. Conversion of light into macroscopic helical motion. Nat Chem 2014;6:229–35.
[321] Ahn S, Ware T H, Lee KM, Tondiglia VP, White TJ. Photoinduced topographical feature development in blueprinted azobenzene-functionalized liquid crystalline elastomers. Adv Funct Mater 2016;26:5819–26.
[322] McConney ME, Martinez A, Tondiglia VP, et al. Topography from topology: photoinduced surface features generated in liquid crystal polymer networks. Adv Mater 2013;25:5880–5.
[323] Wani OM, Zeng H, Wasylczyk P, Priimagi A. Programming photoresponse in liquid crystal polymer actuators with laser projector. Adv Opt Mater 2018;6:1700949.
[324] Yu Y, Nakano M, Ikeda T. Photomechanics: directed bending of a polymer film by light. Nature 2003;425:145.
[325] Lendlein A, Jiang H, Jünger O, Langer R. Light-induced shape-memory polymers. Nature 2005;434:879.
[326] Jiang HY, Kelch S, Lendlein A. Polymers move in response to light. Adv Mater 2006;18:1471–5.
[327] Yamada M, Kondo M, Mamiya J, et al. Photomobile polymer materials: towards light-driven plastic motors. Angew Chem Int Ed 2008;47:4986–8.
[328] Kizilkan E, Strueben J, Staubitz A, Gorb SN. Bioinspired photocontrollable microstructured transport device. Sci Robot 2017;2:eaak9454.
[329] Liu D, Broer DJ. Light controlled friction at a liquid crystal polymer coating with switchable patterning. Soft Matter 2014;10:7952–8.
[330] Chen M, Huang H, Zhu Y, et al. Photodeformable CLCP material: study on photo-activated microvalve applications. Appl Phys A 2011;102:667–72.
[331] Lv J, Liu Y, Wei J, et al. Photocontrol of fluid slugs in liquid crystal polymer microactuators. Nature 2016;537:179–84.
[332] Yamada M, Kondo M, Miyasato R, et al. Photomobile polymer materials – various three-dimensional movements. J Mater Chem 2008;19:60–2.
[333] Cheng F, Yin R, Zhang Y, Yen C-C, Yu Y. Fully plastic microrobots which manipulate objects using only visible light. Soft Matter 2010;6:3447–9.
[334] Palffy-Muhoray P. Liquid crystals: printed actuators in a flap. Nat Mater 2009;8:614–5.
[335] Wani OM, Zeng H, Priimagi A. A light-driven artificial flytrap. Nat Commun 2017;8:ncomms15546.
[336] Zeng H, Wasylczyk P, Wiersma DS, Priimagi A. Light robots: bridging the gap between microrobotics and photomechanics in soft materials. Adv Mater 2017;0:1703554.
[337] Palagi S, Mark A G, Reigh SY, et al. Structured light enables biomimetic swimming and versatile locomotion of photoresponsive soft microrobots. Nat Mater 2016;15:647–53.
[338] Zeng H, Wani OM, Wasylczyk P, Priimagi A. Light-driven, caterpillar-inspired miniature inching robot. Macromol Rapid Commun 2018;39:1700224.
[339] Huang C, Lv J, Tian X, et al. Miniaturized swimming soft robot with complex movement actuated and controlled by remote light signals. Sci Rep 2015;5:17414.
[340] van Oosten CL, Bastiaansen CWM, Broer DJ. Printed artificial cilia from liquid-crystal network actuators modularly driven by light. Nat Mater 2009;8:677–82.
[341] Zeng H, Wasylczyk P, Parmeggiani C, et al. Light-fueled microscopic walkers. Adv Mater 2015;27:3883–7.
[342] Konya A, Gelebart AH, Broer DJ, et al. Making waves in a photoactive polymer film. Nature 2017;546:632.
[343] Yu Y. Materials science: a light-fuelled wave machine. Nature 2017;546:604–6.
[344] Wie JJ, Shankar MR, White TJ. Photomotility of polymers. Nat Commun 2016;7:13260.
[345] White TJ, Tabiryan NV, Serak SV, et al. A high frequency photodriven polymer oscillator. Soft Matter 2008;4:1796–8.
[346] Serak S, Tabiryan N, Vergara R, et al. Liquid crystalline polymer cantilever oscillators fueled by light. Soft Matter 2010;6:779–83.
[347] Lee KM, Smith ML, Koerner H, et al. Photodriven, flexural-torsional oscillation of glassy azobenzene liquid crystal polymer networks. Adv Funct Mater 2011;21:2913–8.
[348] Tang R, Liu Z, Xu D, et al. Optical pendulum generator based on photomechanical liquid-crystalline actuators. ACS Appl Mater Interfaces 2015;7:8393–7.
[349] Yin R, Xu W, Kondo M, et al. Can sunlight drive the photoinduced bending of polymer films? J Mater Chem 2009;19:3141–3.
[350] Kumar K, Knie C, Bléger D, et al. A chaotic self-oscillating sunlight-driven polymer actuator. Nat Commun 2016;7:11975.